A THEORETICAL STUDY OF THE ELECTRON SPIN RESONANCE SPECTRA OF NITROXIDE FREE RADICALS

Thesis by

Martin Stanley Itzkowitz

In Partial Fulfillment of the Requirements

For the Degree of

Doctor of Philosophy

California Institute of Technology

Pasadena, California

1967

(Submitted September 27, 1966)

To My Parents

ACKNOWLEDGMENTS

It is with great pleasure that I express my thanks to the many people who have helped make this work possible. First, I would like to thank Professor Harden M. McConnell for suggesting the problem of nitroxide free radicals and for many invaluable discussions. I would also like to thank my fellow students, especially Drs. Brian M. Hoffman, Arthur W. Merkl, Daniel L. Glaubiger and Zoltán G. Soos for many interesting and helpful suggestions. Particular thanks are due Ralph Young for long and valued hours of discussion.

This thesis would still be unwritten without the constant support and encouragement of my wife, Nancy.

Finally, I would like to thank the National Science Foundation for four graduate fellowships which have financed these years as a graduate student, and the computation centers of the California Institute of Technology and Stanford University for grants of computer time with which these calculations were performed.

ABSTRACT

We are concerned with the electron spin resonance spectra of nitroxide free radicals in various molecular environments. These radicals may be described as a single electron interacting anisotropically with an external field and a nitrogen nucleus of spin one. We use both exact and approximate solutions to the hamiltonian to simulate spectra from oriented samples. We then perform the orientation averages to obtain theoretical spectra from polycrystalline samples. We consider the effects of molecular motion on the system, and develop a Monte Carlo scheme to evaluate the spectrum for a variety of molecular tumbling rates. The theoretical spectra so computed are compared with experimental spectra taken in solutions of varying rotational correlation time; excellent agreement is obtained. We use the Monte Carlo calculation to estimate the rotational correlation time for the molecule in solution.

TABLE OF CONTENTS

I. Introduction

In the recent experimental work of McConnell and co-workers (1-6) it has been found that the attachment of paramagnetic species to large molecules may be used to obtain information about the motion of these molecules. The technique, called "spin-labeling," makes use of the strong dependence of the electron paramagnetic resonance (EPR) spectra of a class of organic free radicals on the motion of these radicals in solution. It is our purpose here to derive theoretical expressions for this dependence, so that one will be able to say with some confidence just how much motion is present in a given sample by looking at its EPR spectrum.

Most of the experimental work done to date has used various forms of nitroxide radicals, shown schematically as I, as the spin label. These radicals are quite

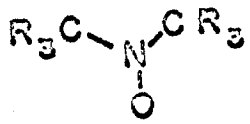

I

stable in solution and exhibit sharp, well-resolved EPR spectra which are qualitatively quite sensitive to molecular motion. These radicals may be synthesized by the

method of Rozantzev and Krinitzkaya (7). Some of these radicals, in particular II and III, have been prepared as

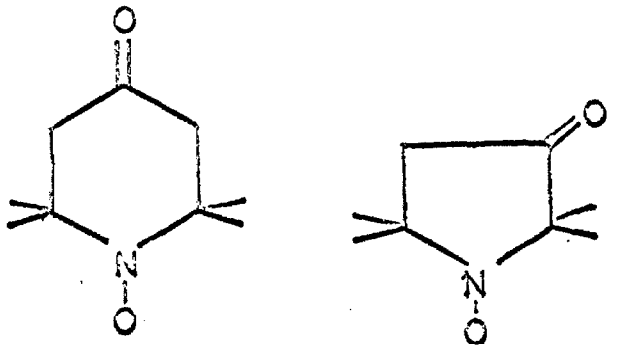

II III

single crystals of their solid solution in tetramethyl-1, 3-cyclobutanedione (8), and their EPR spectra taken as a function of the relative orientation of the crystallographic axes and the external magnetic field. For all orientations, the spectra are well resolved and consist of three lines whose separation is a function of orientation. From these spectra, one may conclude that the hyperfine interaction between the electron (S=1/2) and the nitrogen nucleus (I=1), on which most of the electron spin is presumed to be localized, is anisotropic. Measurement of the position of the central line as a function of orientation leads one to conclude that the g-factor of the electron is dependent on orientation, and must be considered to be a tensor. As far as one can tell from the observed spectra, the g-tensor and the hyperfine tensor have

coincident principal axes. In addition, for the radical IV, the measured hyperfine tensor is axially symmetric.

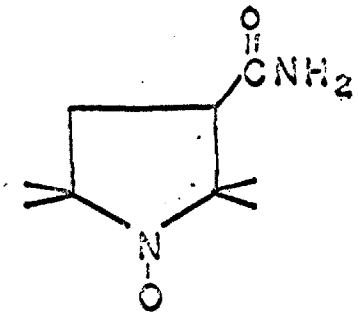

IV

As is to be expected, the anisotropies in the two tensors vary of the order of 20% from compound to compound.

If one prepares a solution of one of these radicals in a nonviscous solvent, the observed EPR spectrum becomes a sharp three-line spectrum, which, of course, is independent of the orientation of the sample in the magnetic field. The observed splittings in such a solution are approximately equal to the average of the three principal axis splittings observed in single crystals, implying that the three principal axis components all have the same sign. If one now increases the viscosity of the solution,* the three lines begin to broaden, with the high field line broadening most rapidly. As one increases the viscosity

---

*The viscosity under consideration is a rotational viscosity of the solution.

of the solution still more, the lines begin to overlap, the spectrum becomes unsymmetric, and the total width of the spectrum approaches the maximum principal axis splitting (3).

Although this viscosity dependence is interesting per se, the main interest in these nitroxide radicals is based on the fact that, if one chooses the R groups in figure I judiciously, one may obtain free radicals that bind to various large molecules of biological interest. If one takes a nitroxide with such a shrewd choice of side group and adds it to a biopolymer which binds to that side group, the spectrum of the product, in nonviscous solution, appears to be the same as the spectrum of the original nitroxide in exceedingly viscous solution. For example, the spectrum of the nitroxide V, with a reactive maleimide

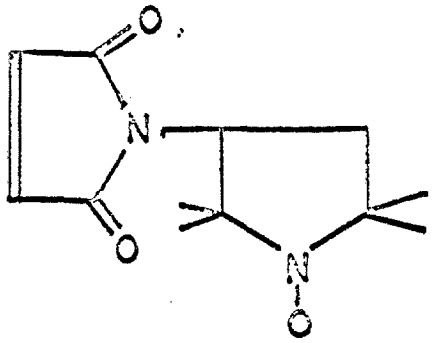

V (Maleimide Reagent)

group, mixed in solution with bovine serum albumin is almost identical to the spectrum of the radical IV in glycerol solution at 77°K (4). In some cases, spectra

corresponding to solutions of intermediate viscosity are obtained. For example, if the nitroxide VI is mixed with

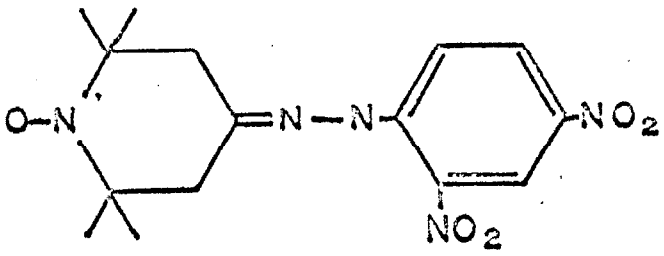

VI (Hapten Nitroxide)

a protein antibody specific to the 2,4-dinitrophenyl group, EPR spectra obtained are quite similar to those of dansyl nitroxide, VII, in 90% glycerol-5% water-5% ethanol solution at 35°C (3).

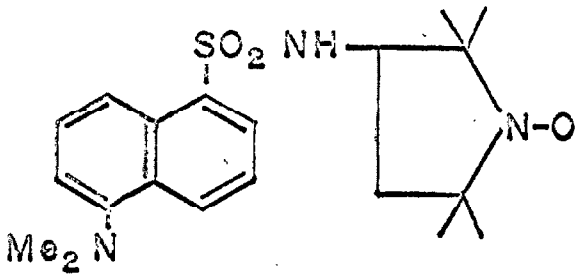

VII (Dansyl Nitroxide)

An experimental technique which has been used to obtain estimates of the extent of molecular motion in a nitroxide from its EPR spectrum is that of Stryer and Griffith (3). In their experiments, the nitroxide VII was prepared; this nitroxide contains both a paramagnetic "spin label" and a "fluorescent label." EPR spectra are

obtained from solutions of the radical in solvents of varying viscosity. For the same solutions the fluorescence depolarization of the dansyl group is measured. From the fluorescence lifetime, τ , the observed emission anisotropy, A, and the emission anisotropy in the absence of all molecular motion, A_o, we may calculate the rotational correlation time, ρ :

$$\rho = 3\tau A/A_o - A \qquad (1.1)$$

For the most part, the theory relevant to the EPR experiments is in rather sad shape. For small deviations from exceedingly rapid tumbling, the theory of Kivelson may be applied (9). The tumbling is assumed isotropic, slow compared to the inverse of the EPR resonance frequency, and fast compared to both the inverse of the mean hyperfine frequency and the inverse of the hyperfine anisotropy. In general, these restrictions are too stringent to allow the theory to be used to fit all of the observed experimental spectra.

The general theories of motional narrowing, in particular those of Kubo (10) and Anderson (11,12) give formal solutions for the EPR line-shapes, but may not be applied to give numerical solutions for the nitroxide problem.

We will here develop a semi-empirical theoretical approach to the problem of the effects of molecular motion on the EPR spectra of nitroxide radicals. We will first discuss the spin hamiltonian that may be used to represent these radicals in the absence of molecular motion. We will show how solutions to this hamiltonian may be obtained; both exact and approximate solutions will be presented, and we will show that for our purposes the approximate solution is sufficiently accurate to enable us to simulate the EPR spectrum. We will show how powder spectra may be obtained from these solutions. We will then consider the most successful of the theoretical approaches to date, that of Anderson, and we will show that the approximations he is forced to make to obtain solutions to his lineshape equations are not valid for the nitroxides under consideration. We will use a crude physical approach to the problem, based on the fact that the EPR experiment implies the existence of a pseudo-stationary state with a lifetime greater than the inverse of the mean hyperfine frequency. We will consider an ensemble of molecules as an ensemble of classical oscillators whose frequency is dependent on orientation; in the presence of motion, the observed frequency will be considered to be the average of all the frequencies sampled by the oscillator in its lifetime. We will use a Monte Carlo method to

perform the above averaging. We will discuss the computer programs that were written to perform all of these calculations, and we will exhibit theoretical spectra and the experimental spectra they are supposed to simulate. We will show that the agreement obtained is quite good. We will correlate our jumping rate to the rotational relaxation time.

In section II, we will discuss the spin hamiltonian, its solutions and the calculation of powder spectra. In section III, we will discuss the formal theory of Anderson, the Monte Carlo method, and our motional approximations. In section IV, we will discuss the computer programs, and in section V, we will compare theory and experiment.

II. The Static Problem

It is presumed that all of the properties of nitroxide free radicals (or any other system for that matter) are contained in the solution to the appropriate exact Schrodinger equation:

$$\mathcal{H}_e \psi_e = i \frac{\partial \psi_e}{\partial t} \tag{2.1}$$

(We set $\hbar = 1$ in the following treatment.)
Given the present state of the art, however, we have little hope of being able to write down the true hamiltonian, much less solve it. We therefore make use of an artifact, known as the spin hamiltonian, $\mathcal{H}$, which depends only on spin operators,* explicit representations for which we can write down, and whose spectrum in the region of interest (here, the EPR region) is believed to be the same as the spectrum of the true hamiltonian.

A. The Spin Hamiltonian and Its Exact Solution

For a single nitroxide radical, in the absence of molecular motion, such a spin hamiltonian may be written:

$$\mathcal{H} = \beta \underline{H}_0^{\dagger} \cdot \underline{\underline{g}} \cdot \underline{S} + \beta_n g_n \underline{H}_0^{\dagger} \cdot \underline{I} + \underline{S}^{\dagger} \cdot \underline{\underline{T}} \cdot \underline{I} \tag{2.2}$$

---

*Strictly speaking, the spin operators in all of the following must be considered to be pseudo-spin operators.

where we have used the following notation:*

$\underline{H}_o$ = the external magnetic field

$\underline{\underline{g}}$ = the electronic g-tensor

β = the Bohr magneton

g_n = the nuclear g-factor for a nitrogen nucleus

β_n = the nuclear magneton

$\underline{S}$ = the electron spin operator (pseudo-spin)

$\underline{I}$ = the nuclear spin operator (pseudo-spin)

$\underline{\underline{T}}$ = the hyperfine tensor

$\underline{\underline{T}}$ here includes both the isotropic Fermi contact interaction and the traceless dipolar coupling term. Since $\underline{\underline{T}}$ is a symmetric quadratic form, there exists a coordinate system in which it may be written as a diagonal dyadic:

$$\underline{\underline{T}} = A\hat{1}\hat{1} + B\hat{f}\hat{f} + C\hat{k}\hat{k} \tag{2.3}$$

Similarly, we may write for $\underline{\underline{g}}$:

$$\underline{\underline{g}} = g_{xx}\hat{i}'\hat{i}' + g_{yy}\hat{j}'\hat{j}' + g_{zz}\hat{k}'\hat{k}' \tag{2.4}$$

where the primed and unprimed axes are not necessarily equivalent. Experimentally, for all of the nitroxides where these tensors have been measured directly, their principal axes do coincide (6,8).

---

*A single underline of a symbol denotes a vector; a double underline denotes a tensor, and a dagger the Hermitian adjoint.

Since S has magnitude 1/2 and I has magnitude 1, we are dealing with a system of six basis states. We may choose a representation of coordinates in which the $\underline{\underline{T}}$ tensor is diagonal, and quantize the z-components of S and I in this coordinate system. The representation so chosen has S^2, S_z, I^2, and I_z as quantum numbers. In this representation, it is straightforward, although tedious, to write down the hamiltonian matrix exactly and explicitly:

(see following page) (2.5)

where we have defined:

$$\underline{H}_e = \beta \underline{\underline{g}} \underline{H}_o \qquad H_e = |\underline{H}_e|$$

$$\underline{H}_n = \beta_n g_n \underline{H}_o \qquad H_n = |\underline{H}_n|$$

A, B, and C are the principal axis values of $\underline{\underline{T}}$ as defined in equation 2.3.

The exact diagonalization of this hamiltonian requires the solution of a sixth order algebraic equation, and hence may not be done in closed form. We observe that if $\underline{\underline{A}}$ is a hermitian matrix of order n which we write as:

$$\underline{\underline{A}} = \underline{\underline{B}} + i\,\underline{\underline{C}} \tag{2.6}$$

where $\underline{\underline{B}}$ is real and symmetric and $\underline{\underline{C}}$ is real and anti-symmetric, the eigenvalues of the supermatrix $\underline{\underline{D}}$:

$$\underline{\underline{D}} = \begin{pmatrix} \underline{\underline{C}} & -\underline{\underline{B}} \\ \underline{\underline{B}} & \underline{\underline{C}} \end{pmatrix} \tag{2.7}$$

$$\mathcal{H} = \begin{pmatrix}
\frac{He_z}{2} + H_{nz} + \frac{c}{2} & \frac{1}{\sqrt{2}}\{H_{nx} - i H_{ny}\} & 0 & \frac{1}{2}\{He_x - i He_y\} & \frac{1}{2\sqrt{2}}\{A-B\} & 0 \\
\frac{1}{\sqrt{2}}\{H_{nx} + i H_{ny}\} & \frac{He_z}{2} & \frac{1}{\sqrt{2}}\{H_{nx} - i H_{ny}\} & \frac{1}{2\sqrt{2}}\{A+B\} & \frac{1}{2}\{He_x - i He_y\} & \frac{1}{2\sqrt{2}}\{A-B\} \\
0 & \frac{1}{\sqrt{2}}\{H_{nx} + i H_{ny}\} & \frac{He_z}{2} - H_{nz} - \frac{c}{2} & 0 & \frac{1}{2\sqrt{2}}\{A+B\} & \frac{1}{2}\{He_x - i He_y\} \\
\frac{1}{2}\{He_x + i He_y\} & \frac{1}{2\sqrt{2}}\{A+B\} & 0 & -\frac{He_z}{2} + H_{nz} - \frac{c}{2} & \frac{1}{\sqrt{2}}\{H_{nx} - i H_{ny}\} & 0 \\
\frac{1}{2\sqrt{2}}\{A-B\} & \frac{1}{2}\{He_x + i He_y\} & \frac{1}{2\sqrt{2}}\{A+B\} & \frac{1}{\sqrt{2}}\{H_{nx} + i H_{ny}\} & -\frac{He_z}{2} & \frac{1}{\sqrt{2}}\{H_{nx} - i H_{ny}\} \\
0 & \frac{1}{2\sqrt{2}}\{A-B\} & \frac{1}{2}\{He_x + i He_y\} & 0 & \frac{1}{\sqrt{2}}\{H_{nx} + i H_{ny}\} & -\frac{He_z}{2} - H_{nz} + \frac{c}{2}
\end{pmatrix} \tag{2.5}$$

of order 2n are simply related to those of $\underline{\underline{A}}$; each eigenvalue of $\underline{\underline{A}}$, a_i, with corresponding eigenvector $\varphi_i = u_i + i\, v_i$, appears twice as an eigenvalue of $\underline{\underline{D}}$, once with eigenvector $\begin{pmatrix} u_i \\ v_i \end{pmatrix}$ and once with eigenvector $\begin{pmatrix} -v_i \\ u_i \end{pmatrix}$ (13). The proof of this theorem follows immediately upon substitution. u_i and v_i are both real.

In those cases where the exact solution to the hamiltonian is required, we form the 12x12 symmetric matrix corresponding to the 6x6 hermitian matrix of the hamiltonian, and diagonalize it numerically by Jacoby's method (14).

After we have obtained the eigenvalues and eigenvectors of the hamiltonian, we may proceed to calculate a theoretical EPR spectrum. In general, the energy level diagram for arbitrary orientation of magnetic field may be pictured as in figure 2.1. (The energy notation in figure 2.1 is defined below.) The nine EPR transitions that may occur are from the three levels of the lower manifold to the three levels of the upper manifold. The three strongest transitions are shown in the figure. In general, we may simulate the full EPR spectrum for an isotropic powder of the nitroxide by using only these three transitions. The worst case we have studied is

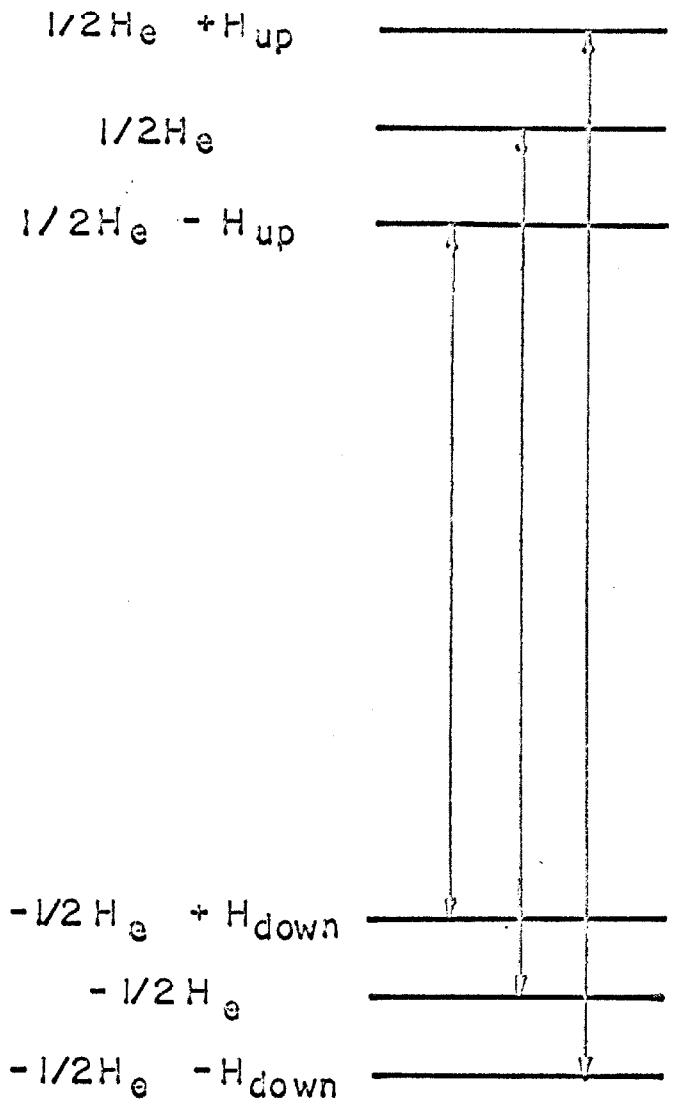

Fig. 2.1. Energy level diagram for a typical nitroxide

that of the radical chlorpromazine, VIII, at Q-band

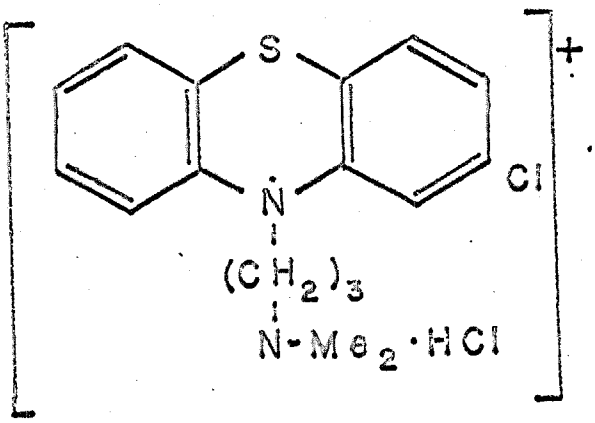

VIII (Chlorpromazine Radical-ion)

(12,400 gauss for H_o). The six forbidden transitions there become as much as 20% as strong as the three main transitions. Even for this compound, however, the weak transitions do not affect the composite powder spectrum. This is discussed in more detail in section V.

The transition moment for an EPR transition is proportional to the square of the matrix element of the magnetic moment perpendicular to the external field between the two states of the transition. This magnetic moment is proportional to the perpendicular component of $\underline{\underline{g}}\underline{S}$; since $\underline{\underline{g}}$ is anisotropic one would expect the transition intensity to be a function of the particular perpendicular component selected. However, the anisotropies in $\underline{\underline{g}}$ are only of the order of 1 part in 1000, so the resultant difference in intensities should vary by only 1 part in

10^6; we may neglect this variation, and, in fact, take our relative intensities as the ratios of the squares of the matrix elements of $S_\perp$ for the transitions.

We write the magnetic field in the coordinate system in which $\underline{\underline{T}}$ is diagonal:

$$\underline{H}_0 = H_0 \begin{pmatrix} \sin\theta\sin\varphi \\ -\sin\theta\cos\varphi \\ \cos\theta \end{pmatrix} \tag{2.8}$$

where theta and phi are the standard polar coordinates of the principal z-axis of the $\underline{\underline{T}}$ tensor measured from the external field. We then choose for our transition moment the matrix element of $S_\perp^*$:

$$S_\perp^* = \cos\varphi\, S_x + \sin\varphi\, S_y \tag{2.9}$$

For any other choice of perpendicular component, the transition matrix element differs from ours by a change in phase; the transition moment is unaffected. Our choice is dictated by ease of computation. We evaluate this matrix element over the exact (numerical) eigenstates of the hamiltonian.

For an arbitrary orientation of the magnetic field, the solution of the hamiltonian and the evaluation of the nine possible transition moments is a time-consuming process: on an IBM 7090 computer, which is the computer on which all of our calculations were performed, using the

programs described in section IV, approximately 3 seconds is required for each orientation. In order to simulate a powder spectrum (see below) a minimum of 600-1000 orientations must be used. We therefore decided to use some form of approximate solution to the hamiltonian.

B. The Approximate Solution

Writing our hamiltonian 2.2 in the coordinate system in which $\underline{\underline{T}}$ is diagonal, we let:

$$\underline{H_e} = H_e \hat{\underline{u}} \qquad \hat{\underline{u}} = \underline{H_e} / H_e \tag{2.10}$$

We define $\underline{\underline{B}}$ as that transformation matrix such that:

$$\underline{\underline{B}} \cdot \underline{H_e} = H_e \begin{pmatrix} 0 \\ 0 \\ 1 \end{pmatrix} \tag{2.11}$$

We may then rewrite our hamiltonian as:

$$\mathcal{H} = H_e S_z' + \underline{H_N}^{\dagger} \cdot \underline{I}' + \underline{S}'^{\dagger} \underline{\underline{T}}' \cdot \underline{I}' \tag{2.12}$$

where

$$\underline{S}' = \underline{\underline{B}}\,\underline{S}$$

$$\underline{I}' = \underline{\underline{B}}\,\underline{I}$$

$$\underline{H_N} = \underline{\underline{B}}\,\underline{H_n}$$

$$T' = \underline{\underline{B}}\,\underline{\underline{T}}\,\underline{\underline{B}}^{-1}$$

Define $S_{\parallel}$ and $\underline{S}_{\perp}$ as follows:

$$S_{\parallel} = S_3'$$
$$\underline{S}_{\perp} = \begin{pmatrix} S_x' \\ S_y' \\ 0 \end{pmatrix} \tag{2.13}$$

we rewrite the hamiltonian as:

$$\mathcal{H} = \mathcal{H}_e + \mathcal{H}_1 + \mathcal{H}_2 + \mathcal{H}' \tag{2.14}$$

with:

$$\mathcal{H}_e = H_e S_{\parallel}$$
$$\mathcal{H}_1 = (\tfrac{1}{2} + S_{\parallel}) \left\{ \underline{H}_N^{\dagger} + \tfrac{1}{2}(T_{31}', T_{32}', T_{33}') \right\} \cdot \underline{I}'$$
$$\mathcal{H}_2 = (\tfrac{1}{2} - S_{\parallel}) \left\{ \underline{H}_N^{\dagger} - \tfrac{1}{2}(T_{31}', T_{32}', T_{33}') \right\} \cdot \underline{I}'$$
$$\mathcal{H}' = \underline{S}_{\perp}^{\dagger} \cdot \underline{\underline{T}}' \cdot \underline{I}'$$

We will now diagonalize the first three terms of the hamiltonian 2.14 exactly, and show that the perturbation expansion of the fourth term gives very small corrections.

We use eigenfunctions of $S_{\parallel}$ for our electronic basis functions. The eigenvalues of $S_{\parallel}$ are $\pm 1/2$; therefore, for each state, one of the terms $\mathcal{H}_1$ or $\mathcal{H}_2$ must vanish. We define the unitary matrices A_1 and A_2 by:

$$\left\{ \underline{H}_N^{\dagger} + \tfrac{1}{2}(T_{31}', T_{32}', T_{33}') \right\} \cdot \underline{\underline{A}}_1 = (0, 0, H_{up}) = \underline{H}_{up}^{\dagger}$$
$$\left\{ \underline{H}_N^{\dagger} - \tfrac{1}{2}(T_{31}', T_{32}', T_{33}') \right\} \cdot \underline{\underline{A}}_2 = (0, 0, H_{down}) = \underline{H}_{down}^{\dagger} \tag{2.15}$$

Let $\underline{A}_1\underline{I}' = \underline{I}_{up}$ and $\underline{A}_2\underline{I}' = \underline{I}_{down}$. We choose the following representation for the six basis states of the system: the electronic basis functions are eigenstates of $S_\parallel$; when the eigenvalue of $S_\parallel$ is +1/2 we choose eigenstates of the z-component of $\underline{I}_{up}$ for the nuclear states; when the eigenvalue of $S_\parallel$ is -1/2, we choose eigenstates of the z-component of $\underline{I}_{down}$. We may readily verify that the hamiltonian 2.14 with the deletion of the fourth term is diagonal in this representation. We now consider the effect of $\mathcal{H}'$. Since $\mathcal{H}'$ involves only S_x' and S_y' it has no diagonal matrix elements for any of the six basis states. To first order, therefore, our full hamiltonian is diagonal. The utility of this approximation is predicated on the inequalities $H_e \gg H_N, A, B, C$. We may therefore speak unambiguously of an upper and lower manifold as in figure 2.1. Since the states in a manifold, which have relatively small energy separations, all have the same eigenvalue of $S_\parallel$, $\mathcal{H}'$ connects only those states which are in different manifolds. The second order corrections to the energies are therefore only those terms that have energy denominators of the order of H_e. The matrix element of $\mathcal{H}'$ between such connected states is of the order of the x or y hyperfine component; the energy corrections are therefore of the order of 0.1 MH for typical nitroxides at X-band (3350 gauss; 9KMH). These contributions are negligible, and are thrown out in the numerical calculation. We do observe,

however, if the nuclear Zeeman field becomes approximately parallel to and equal in magnitude to the hyperfine field, the nuclear splittings in the resultant field $\underline{H}_{down}$ become exceedingly small; in this case, corrections of order higher than second become important and the approximation breaks down. The only case in which this occurs in practice is in the calculation of the spectrum of chlorpromazine at Q-band. Single orientation spectra calculated by this approximation scheme differ markedly from those calculated by exact diagonalization.

As before, we now proceed to calculate transition moments, this time using our approximate eigenfunctions. We choose S_x' as the transition moment operator; S_x' connects only states in different manifolds, and acts only on the electronic part of the wave function. The transition matrix element therefore depends linearly on the overlap between the nuclear states, one quantized along $\underline{H}_{up}$ and the other quantized along $\underline{H}_{down}$. We define:

$$\cos\Theta = \underline{H}_{up}^{+}\,\underline{H}_{down} / H_{up} H_{down} \qquad (2.16)$$

If we consider $\underline{I}_{up}$ to be quantized along a "z" axis then $\underline{I}_{down}$ eigenstates are quantized along an axis related to this "z" axis by a rotation of Θ about the x-axis; we may therefore trivially write the overlap matrix in terms of the rotation matrix for angle Θ. This overlap matrix is:

$$\sum_{\underline{\underline{m}}} = \frac{1}{2} \begin{pmatrix} 1+\cos\Theta & \sqrt{2}\sin\Theta & 1-\cos\Theta \\ -\sqrt{2}\sin\Theta & 2\cos\Theta & \sqrt{2}\sin\Theta \\ 1-\cos\Theta & -\sqrt{2}\sin\Theta & 1+\cos\Theta \end{pmatrix} \qquad (2.17)$$

Figure 2.2 shows the relationship between the various real and pseudo-fields used in this approximation.

We have now seen how we may calculate the EPR spectrum of a nitroxide radical as a function of orientation. For any orientation, there are nine possible transitions; three of these are strong. None of the other six lines have been seen experimentally. The case where one would expect these to be strong has not been studied. When the field is aligned along an axis of symmetry in the $\underline{\underline{T}}$ tensor, all but one of the six forbidden lines vanish exactly.

Theoretically, the spectrum we have predicted above should have infinitely sharp lines. In practice, of course, the lines are not this sharp. They are (in single crystal solid solution) gaussian in shape and approximately four guass wide (8). We will, in this work, take this residual linewidth as an input parameter, much in the same way as we take the $\underline{\underline{g}}$ and $\underline{\underline{T}}$ tensors as experimentally determined. The residual linewidth is presumably due to many factors. Interaction between spins on different radicals and residual hyperfine interaction with neighboring protons both contribute. For the region of motional speeds we consider below, the linewidth is reasonably independent of tumbling

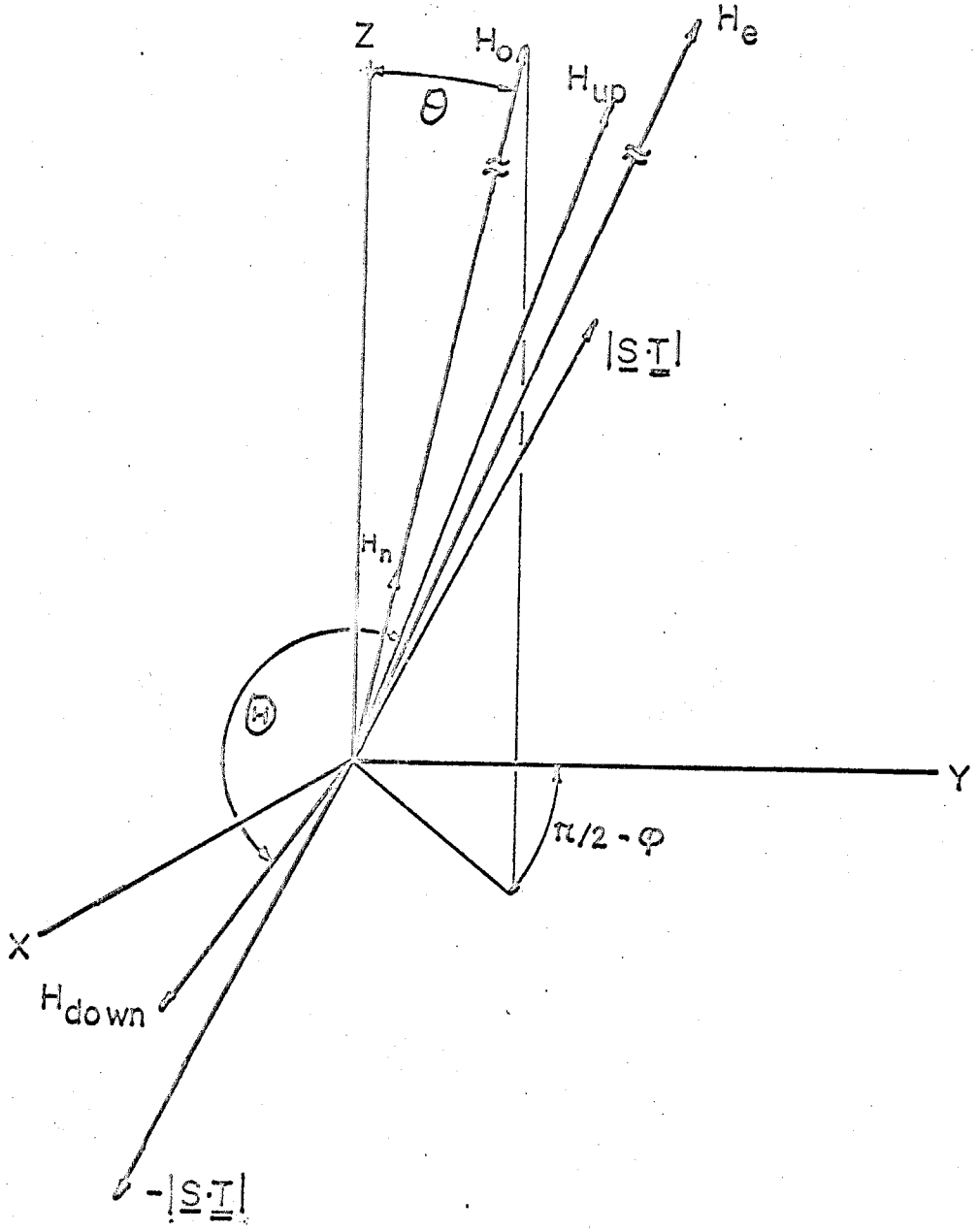

Fig. 2.2. The various fields and pseudo-fields defined in the text

rate (as determined by comparison of our theoretical spectra with the experimental spectra). In a rigid glass the linewidth is about five gauss; in a nonviscous solvent with almost free rotation the linewidth is of the order of two gauss. We may attribute this difference to the averaging out of the anisotropic contribution to the proton hyperfine interaction.

C. Spectra from Polycrystalline Samples

Unfortunately for the experimentalist, it is often quite difficult to prepare crystals in which all the paramagnetic species have the same orientation, so that one may measure the anisotropies on $\underline{\underline{T}}$ and $\underline{\underline{g}}$ directly. Single crystals of biomolecules are especially difficult to prepare, and here one must usually be content with polycrystalline or solution samples. (The notable exception to this is the work of Ohnishi, Boeyens, and McConnell on haemoglobin (6).) We will now consider the resonance spectrum expected from a polycrystalline sample of nitroxide radicals.

We regard the molecules as independent, so that the total hamiltonian for the sample may be written as the sum of single radical hamiltonians:

$$\mathcal{H} = \Sigma \mathcal{H}_i \qquad (2.18)$$

If this approximation is made, the spectrum of the system reduces to a linear superposition of the spectra of the individual radicals. If $I_i(\nu)$ is the spectral density function for the i^{th} molecule, and $I(\nu)$ is the polycrystalline spectral density, we write:

$$I(\nu) = \sum I_i(\nu) \tag{2.19}$$

(In accordance with the theory developed above, each $I_i(\nu)$ may be written as the sum of three gaussians, one for each of the principal lines, and the six gaussians for the near-vanishing forbidden transitions.)

We make the assumption of a large number of individual molecules, with a distribution in orientation of $\rho(\theta,\varphi)$, and transform the sum 2.19 to an integral over orientation space:

$$I(\nu) = \int I_{\theta,\varphi}(\nu)\, \rho(\theta,\varphi)\, d\theta\, d\varphi \tag{2.20}$$

where $I_{\theta,\varphi}(\nu)$ is the spectral distribution function for a molecule with orientation θ,φ relative to the external field. The equation 2.20 is quite general; by specifying various forms for the orientation distribution, we may simulate various types of spectra. If we set ρ equal to a delta function at a particular orientation, we may generate the spectrum of a single crystal doped with nitroxide radicals; if we choose ρ as $\sin\theta$, we simulate an isotropic powder or rigid glass. By an appropriate choice

of ρ we may also use this expression to simulate spectra where the molecules are oriented by flow (1).

The practical use of equation 2.20 requires that we express the spectral distribution function $I_{\theta,\varphi}(\nu)$ in closed form as a function of orientation, and that we can do the integral over orientation. We cannot hope to do this in practice; we therefore map the surface of the orientation sphere onto a grid in θ,φ space, and convert the integral over this surface, to a sum over grid points:

$$I(\nu) = \sum_{i,j} I_{\theta_i \varphi_j}(\nu)\rho(\theta_i, \varphi_j) \qquad (2.21)$$

where we have made the necessary continuity assumptions on the functions I and ρ . The accuracy of equation 2.21, of course, depends on the size of our grid. We found that a grid of 32x32 points for the half-sphere was adequate for all the experimental spectra simulated. Note that we need only consider the half-sphere because our hamiltonian is invariant under inversion. For some cases, a grid of 25x25 points was found sufficient.

Having discussed the static hamiltonian and obtained its solutions and the EPR spectra predicted from them, we are now prepared to consider the effects of molecular motion on the spectrum.

III. The Effects of Motion on the Spectrum

The formalism developed in the previous section is based on the implicit assumption that the hamiltonian is time-independent, that is, that the spins undergo no motion in times of the order of the duration of the EPR experiment. (By motion, of course, we mean only motion which does not commute with the spin hamiltonian; translation of the spins, which does commute, may occur, but will not affect the spectrum.) For this to be true the spins must be rigidly bound against rotation, as indeed they are presumed to be in rigid glass or rigidly bound spin-labeled compounds. Experimentally, this situation, although common, is not the situation of prime importance. We must therefore consider the intrinsically more interesting case where the spins do execute some form of more or less rapid motion, and we must try to calculate the effect of such motion on the observed EPR spectrum.

A. The Theory of Anderson (11,12)

The earliest work on motional effects in magnetic resonance spectra is that of Bloembergen, Purcell and Pound (15). They consider the nuclear resonance spectrum in a magnetic field which is composed of a static,

externally applied field, $\underline{H}_o$, and a random local perturbation which depends on the neighbors of the particular spin under consideration:

$$\underline{H}_i = \underline{H}_o + \sum_j \frac{1}{r_{ij}^3} (\underline{1} - 3\hat{r}\hat{r}) \cdot \underline{\mu}_j \qquad (3.1)$$

The second term (local field) is taken as a dipole field, and is presumed much smaller than the external field. Although the motion of the spins does not directly affect their resonance spectrum, it does serve to vary, in a "random" fashion, the dipolar field. Physically, it is evident that, as the motion becomes more and more rapid, the broadening effect of the local field will be averaged out. If, in the absence of motion, the observed resonance line has a mean square width, ΔW,

$$\Delta W = \langle w^2 \rangle^{1/2} \qquad (3.2)^*$$

in the presence of motion with characteristic frequency, w_m, this width is reduced to approximately w^2/w_m.

Anderson and Weiss (11) and Anderson (12) have developed a theory of motional and exchange narrowing of spectral lines which puts these results on a somewhat sounder theoretical basis. Their theory also accounts for the results of Van Vleck and Van Vleck and Gorter (16) on

---

*Frequencies are measured from the position of the zero-order line.

exchange narrowing. The full hamiltonian for the problem is written as the sum of three terms:

$$\mathcal{H} = \mathcal{H}_0 + \mathcal{H}_b + \mathcal{H}_m \tag{3.3}$$

where $\mathcal{H}_0$ is the zeroth order hamiltonian for the spins, $\mathcal{H}_b$ is the broadening perturbation, and $\mathcal{H}_m$ is the motional contribution to the hamiltonian. The key assumption made by Anderson is that the motional term of the hamiltonian has no direct effect on the spectrum; for this to be true we must have:

$$\begin{aligned} [\mathcal{H}_m, \mathcal{H}_0] &= 0 \\ [\mathcal{H}_m, \underline{\mu}] &= 0 \end{aligned} \tag{3.4}$$

where $\underline{\mu}$ is the magnetic dipole moment of the system. However, for $\mathcal{H}_m$ to have any effect at all, it cannot commute with the broadening perturbation; $\mathcal{H}_m$ is therefore seen to modulate this broadening perturbation. In the problem considered by Anderson, the g-factor for the resonant spins is assumed isotropic, the zeroth order term to be the isotropic Zeeman interaction, and the broadening term to be a spin-spin dipolar coupling between the various resonant spins of the ensemble. It may be readily verified that equations 3.4 are satisfied for this system, since neither $\mathcal{H}_0$ nor $\underline{\mu}$ has any spatial dependence.

In order to make his problem tractable, Anderson first assumes the broadening perturbation to be a discrete set of frequency shifts; in the absence of motion then,

the spectral distribution function for the absorption may be written:

$$\underline{I}(\nu) = \sum P_i I_i(\nu) = \underline{P} \cdot \underline{I}(\nu) \qquad (3.5)$$

where P_i is the intrinsic probability of a given spin having its resonance frequency shifted by W_i, with a corresponding spectral distribution $I_i(\nu)$. For the case of exchange narrowing, the random motion is considered to be gaussian; for true motional narrowing, the motion is considered to be Markoffian. (These are the only two types of random functions that may be conveniently handled.) We are concerned only with the motional part of his theory.

The motion has been assumed to be Markoffian, that is, the probability of a spin being in state i (of the perturbation) at time t, given that it was in state j at time $t-\Delta t$, is independent of its state for all times earlier than $t-\Delta t$. The motion is assumed smooth, so that we may linearize the Markov transition matrix, $\underline{\Omega}$, for small times, τ:

$$\underline{\Omega} = \underline{1} + \tau \underline{\Pi} \qquad (3.6)$$

where $\underline{1}$ is a unit matrix and $\underline{\Pi}$ is a transition probability matrix. From this expression and the definition of the correlation function $\varphi(\tau)$, we may obtain the correlation function:

$$\varphi(\tau) = \underline{P}^{\dagger} \left(\exp\left[\tau\left(i\underline{\omega} + \underline{\Pi}\right)\right]\right) \cdot \underline{1} \qquad (3.7)$$

where $\underline{1}$ is a column vector with all entries unity, $\underline{P}$ is the vector of initial probabilities as in equation 3.5, and $\underline{\underline{\omega}}$ is a diagonal matrix with $\omega_{ij} = \omega_i \delta_{ij}$. We then find a transformation matrix, $\underline{\underline{T}}$, such that the matrix $\underline{\underline{T}}^{-1}(i\underline{\underline{\omega}} + \underline{\underline{\Gamma}})\underline{\underline{T}}$ is diagonal. If we then take the fourier transform of the correlation function, which is now a sum of complex scalar exponentials, we obtain a spectral density function which is a sum of Lorentzians; the negative real part of each of the eigenvalues of the matrix $i\underline{\underline{\omega}} + \underline{\underline{\Gamma}}$ gives the width of the corresponding Lorentzian, the imaginary part the shift.

Formally, we may readily extend this treatment to a broadening perturbation which has a continuous distribution of frequencies. The eigenvalue equation which determines the position and width of the Lorentzian lines becomes an integral equation. If the assumption that the Markov transition matrix depends only on the second subscript (that is, that the frequency after the transition is completely uncorrelated with the frequency before the jump) can be made, then the integral equation admits of solution in the limiting cases of infinitely rapid motion and infinitely slow motion. An attempt to treat less or more rapid motion, respectively, by a perturbation expansion is successful only in the former case; the solutions for zero motion are singular. For the gradual slowing

down of the motion, results in accordance with equation 3.2 are obtained.

Let us now try to apply the theory developed above to the problem of motion in nitorxide spectra. In this case, we may neglect the inter-molecular dipolar and exchange contributions to the broadening: the spectra are taken in dilute solution. We consider the entire broadening to be attributable to the anisotropies in the $\underline{\underline{g}}$ and $\underline{\underline{T}}$ tensors. As mentioned above, translational motion commutes with the entire spin hamiltonian, and is therefore of no interest. We consider only rotational effects.

Anderson's theory is designed to treat only a single spectral line broadened by some perturbation. In the limit of infinitely rapid motion he must, therefore, obtain a single infinitely sharp line for the spectrum. The nitroxide radicals, however, exhibit three-line spectra for all speeds of motion: no motion may average out an isotropic interaction. If we wish to apply this theory, we must consider the three hyperfine states to be independent, that is, unmixed by the motion. This is not a particularly serious fault, and, in fact, we will make this approximation in our own treatment. We then may use the isotropic part of the hamiltonian as $\mathcal{H}_o$. The broadening part of the hamiltonian is obviously the anisotropic parts of the $\underline{\underline{g}}$ and $\underline{\underline{T}}$ tensor terms.

The motional part of the hamiltonian does commute with $\mathcal{H}_0$ so that the first equation of 3.4 is satisfied; however, the magnetic moment of the system does depend on the anisotropic $\underline{g}$-tensor, and hence will not commute with the motion. The commutator of the second equation 3.4 will not be identically zero, even though it will be small. The expression for the correlation function will no longer just depend on the frequency distribution of the broadening, but will contain other terms coming from the time dependence of the magnetic moment. Neglecting this, we are still faced with the fact that the broadening spectrum is continuous. We are hard pressed to believe the assumption that the frequencies before and after a transition are completely uncorrelated, since in our case the transition frequencies are smoothly varying with orientation, not randomly fluctuating, and the motion is best considered as a small-step random walk in orientation. So we see that Anderson's lineshape equations cannot be solved for a nitroxide radical, except by making some rather untenable assumptions.

Any a priori theoretical treatment of the motion would have to be based on an explicit hamiltonian for this motion. At present, we cannot write down such a hamiltonian; we therefore look for an intuitive physical approach to the problem of motional averaging.

B. Our Hypothesis

We know that for the highest rotational speeds considered here, the spectrum of a nitroxide radical consists of three sharp lines. Similarly, at the slowest speeds (that is, no motion at all) the spectrum of a single radical consists of three well-resolved lines (we here neglect the forbidden transitions). The separation of these lines is of the order of the mean hyperfine frequency, $\bar{a}$. By virtue of the uncertainty relation in the energy,

$$\frac{1}{\Delta t} < \Delta E = \frac{1}{3} \mathrm{Tr}(\underline{T}) = \bar{a} \qquad (3.8)$$

we must be able to regard the system as being in a pseudo-stationary state for times, Δt, at least as long as the inverse of the mean hyperfine frequency: for, if this is not true, we would not be able to resolve the hyperfine lines. We now ask ourselves what parameters, in particular, what transition frequencies, may we use to describe this pseudo-stationary state. The obvious answer is found in the following semi-classical treatment:

Let us suppose that at time t=0 the molecule is in a particular eigenstate of the spin hamiltonian corresponding to its instantaneous orientation θ, φ. During every interval of time, τ, the molecule undergoes a collision with solvent and takes a small random step to some neighboring orientation, and is now in a state with transition

frequency $\nu(t)$. This is reasonable assumption for the motion of the spin if the nitroxide molecule is so large compared to a solvent molecule that it may be regarded classically (Debye limit). We then say that the observed EPR transition frequency for the pseudo-stationary state is the average of all the frequencies the molecule has sampled in the time Δt:

$$\nu^{obs} = \frac{\tau}{\Delta t} \sum_{j=0}^{\Delta t/\tau} \nu(t+j\tau) \qquad (3.9)$$

We know that equation 3.9 reduces to the right limit in the absence of motion, that is, the observed resonance frequency is equal to the instantaneous resonance frequency. If we assume that the hyperfine states are not mixed by the motion (see below) we see that equation 3.9 reduces to the right limit for very rapid motion as well. Our thesis here is that this equation is valid for all intermediate cases. This is only an assumption. We cannot justify it rigorously; however, we will show that the theoretical spectra generated under this hypothesis are in very close agreement with experimental spectra.

We must now consider a method for determining the instantaneous frequencies that appear in the average 3.9. We will make the assumption that the electron and nuclear states are not mixed by the sudden jumping. In a sense, we may consider this as having the spins follow their own

instantaneous fields adiabatically. On the face of it this assumption is difficult to justify a priori. Even if we think of the physical motion as not a real random walk, but rather a fairly smooth rotation, whose direction is changed by the solvent collisions, the molecule does sample the orientations very rapidly. So one might think that each change will induce a certain probability of transition between the various nuclear states, and the molecule will rapidly forget which hyperfine state it started in. Part of the damage of these transitions is undone by the fact that a two-dimensional random walk is self-intersecting infinitely often: if we return to a given position in a time short compared to the energy separation of eigenstates, so that the component states after jumping have not had a chance to get out of phase, we will return to our starting state again. For the energies of the various intermediate states the molecule has visited, we use the expectation of the instantaneous hamiltonian over the starting eigenstate. We will assert that the rate of transition between the various hyperfine states is small, so that the starting eigenstate is probably not very different from the instantaneous eigenstates. We may therefore approximate the energy expectation by the eigenvalue of the instantaneous hamiltonian for the corresponding eigenstate.

We will now develop the methods used for performing the random walk and calculating the average transition frequency.

C. The Monte Carlo Method

"One of the main strengths of theoretical mathematics is its concern with abstraction and generality: one can write down symbolic expressions of formal equations which abstract the essence of a problem and reveal its underlying structure. However, this same strength carries with it an inherent weakness: the more general and formal its language, the less is theory ready to provide a numerical solution in a particular application" (17). Presumably when we write down the Schrodinger equation as in equation 2.1 we have solved the problem. But we are here concerned not so much with a formal and general solution as with a numerical result: we wish to be able to simulate the experimental spectra. We must now consider the numerical techniques that may be used to obtain solutions to equation 3.9.

Our first concern is with the derivation of a method for generating the random walk that each molecule is presumed to undergo. For this, we will use the Monte Carlo method. We first consider the direct Monte Carlo simulation of a random process.

Suppose we have a random process, with possible outcomes E_1, E_2, E_3, ... E_n, with corresponding probabilities P_1, P_2, P_3, ... P_n, where

$$\sum_{i=1}^{n} P_i = 1 \tag{3.10}$$

We will divide the unit line into segments of length P_1, ... P_n as shown in figure 3.1. Suppose we have at our disposal a means of generating a random number, R, whose distribution function is uniform on the unit line. We then simulate our random process by saying that for this trial, event E_1 occurs if the random number is in the first segment, event E_2 if the random number is in the second segment, etc.; that is, event E_i occurs if:

$$\sum_{j=1}^{i-1} P_j \leq R < \sum_{j=1}^{i} P_j \tag{3.11}$$

If the series of random numbers we generate does have a uniform distribution on the unit line, the effect of the simulation of the random process will asymptotically approach the effect of the process itself.

A second technique that is referred to as the Monte Carlo method is the technique of using a random process to simulate a determined process which cannot be solved in closed form. This technique is usually called

Fig. 3.1. Division of the unit line for a Monte Carlo simulation of a random event

"sophisticated Monte Carlo." A typical example of this might be the evaluation of a multidimensional integral over a function which is not integrable in closed form. The standard numerical technique for such an integral is to divide the region of integration into some form of grid, uniform in the crudest approximation, and evaluate the function at each of the grid points and perform the direct sum. If we use a uniform net in n dimensions with N points for each dimension, it may be shown (17) that the limit of accuracy for the integral is N^{-1}.

We now consider the same problem from the point of view of sophisticated Monte Carlo: We generate an n-dimensional random vector, each of whose components is uniform over the interval of integration of the corresponding variable of integration. We then evaluate the function at the point corresponding to the random vector, generate a new point and proceed until we have generated N^n points. We sum all the contributions and find that the rate of convergence of our approximation to the integral is $N^{-n/2}$. In other words, for n large, we need generate fewer points, and hence evaluate the integrand fewer times, if we choose the integration points at random rather than by a preset grid (for a given degree of accuracy). In addition, if the integrand is sufficiently perverse, the Monte Carlo method may be the only way of obtaining a convergent approximation to the integral.

The utility of the two Monte Carlo methods discussed above obviously depends on having at one's disposal a quick and clean method for generating a sequence of random numbers with a given distribution function. The quick is necessary so that you don't lose the efficiency gained by an enhanced convergence rate in the time spent evaluating the integrand at the points of the sum. The clean is necessary so that the distribution of random numbers chosen does not contain any bias, and, hence, will not weight one region of space more heavily than another.

The obvious choice for a random number generator would be a random physical system, a sort of inverse Monte Carlo. For example, one might use the last few digits of the random noise voltage in a resistor, or any of a large series of physical processes which have some inherent fluctuating noise. These methods are discussed in some detail in the book by Shreider (18). In general, however, physical generators of random numbers are slow, and not particularly well suited for use with high-speed digital computers, such as the IBM 7090 on which we perform all our calculations.

We will take refuge in the use of pseudo-random numbers. Pseudo-random numbers are numbers which are generated by some deterministic process, yet which are believed to satisfy all of the statistical tests for

randomness required in the particular application. The use of pseudo-random numbers is always somewhat of a risk: you may not have thought of the right statistical criterion the numbers are assumed to satisfy, but don't. Indeed, Von Neumann, one of the originators of the Monte Carlo method, has characterized anyone using deterministic "random numbers" as being in "a state of sin" (19). However, with gay abandon, we will use pseudo-random numbers for our calculation.

There are currently in vogue three main methods for generating series of pseudo-random numbers (20). These are the Von Neumann mid-square technique where the n+1st random number is generated from the n^{th} by squaring and extracting the middle digits, the multiplicative-congruential method with the recursion relation:

$$R_{n+1} \equiv a R_n \pmod{m} \tag{3.12}$$

and the mixed congruential method with recursion relation:

$$R_{n+1} \equiv a R_n + c \pmod{m} \tag{3.13}$$

In the above two methods, a, c, and m are constants, with m usually depending on the hardware of the actual computer the numbers are being used with. For the IBM 7090, with a fixed word length of 35 bits, any method of generating pseudo-random numbers must repeat itself in 2^{35} or fewer terms. A careful choice of the parameters in equations 3.12

or 3.13 will enable us to generate a sequence of pseudo-random numbers with period very nearly approaching this. For our work, we will use the multiplicative-congruential method, equation 3.12, with $m=2^{35}$ and R_o and a both equal to 5^{15}. This sequence can be shown to have period of the order of 10^{10}, which is more than ample for our needs, to have very little serial correlation, and to take only 8 microseconds for each number required. We will now consider the way in which the Monte Carlo method can be used to generate theoretical nitroxide spectra as a function of molecular motion.

D. Simulation of Nitroxide Spectra

We will first consider the simulation of a spectrum due to a single nitroxide molecule undergoing a random walk of N steps in a time equal to its EPR lifetime (the Δt of equation 3.8). Suppose that the molecule starts at a particular orientation θ_o, φ_o with respect to the external field. We have divided the surface of the sphere into a grid in both θ and φ as implied in equation 2.21, in the discussion of powder spectra. We assume the molecule is in one of the three hyperfine states (actually, one of the three pairs of states whose energy differences are the three strong transitions of the spectrum). For each jump, we will allow the molecule to move to one of the four neighboring grid points. This squared-off motion is perhaps

not the most reasonable of approximations: we really should consider the molecule to jump to any of the continuum of states with a given increment of angle from the starting states. We are confident, however, that the particular form of motion we constrain the molecule to undergo will not affect the spectrum; this should be true whenever the motion is such that the orientation after very long times is uncorrelated with the orientation at time t=0.

One of the problems we must consider is an artificial one introduced by our particular choice of grid. If we divide the angles ϑ and φ into equally spaced divisions, we will obtain a distribution of grid points that is clustered around the poles. We will counteract this clustering by assigning a weight function, proportional to the sine of the theta for a given point, to the intrinsic probability of a given orientation. Similarly, we must avoid this orientation bias in our jumping algorithm. We assure the statistical independence of final and initial orientations by biasing the probabilities of jumping into a state with a given theta by the sine of that theta; that is, for jumps to the two neighboring points differing in the theta coordinate, we assign the relative probabilities of increasing and decreasing theta by one unit of grid spacing, δ :

$$\frac{P_+}{P_-} = \frac{\sin(\theta+\delta)}{\sin(\theta-\delta)} \tag{3.14}$$

We still must consider the relative probabilities of changing theta and phi. (It is evident that the probabilities of increasing and decreasing phi, given that the jump is in the phi direction, are both 1/2.) Clearly, the transition probabilities for all four neighboring configurations are 1/4 for jumps from the equator. Since we determine the relative probabilities of increasing theta and decreasing theta by statistical equilibrium considerations, the ratio of the probabilities of changing theta and phi must be independent of theta; we therefore say that the molecule has a 50 per cent chance of changing theta and a 50 per cent chance of changing phi.

This determination of the probabilities for jumping in various directions completes our discussion of the spectrum of a single nitroxide radical in the presence of molecular motion. Of course, we may obtain no equivalent to single crystal spectra in the presence of motion. We therefore must use the formalism of section II C.

We may represent the spectrum of a macroscopic sample of nitroxide in the presence of motion formally by equation 2.19; when we transform this sum over individual molecules into a sum over orientations, we must also include the effects of varying path, Ω :

$$I(\nu) = \sum_{j,k,\Omega} I_{\theta_j,\varphi_k,\Omega}^{(\nu)} \rho(\theta_j^*, \varphi_k^*) \qquad (3.15)$$

We have no hope of obtaining this sum in closed form. We therefore resort to a Monte Carlo technique for evaluating it. We leave the expression for the resultant lineshape of the sample as a sum over individual molecules. We then choose a single molecule in a random orientation and allow it to execute the random walk described above, and, after the required number of steps has been taken, we average the frequency of the molecule, and add it to our sum. In practice, for each of the molecules so simulated, we average all three hyperfine frequencies over the same motion. This should not bias the resultant spectrum in any way, and affords a ready means of decreasing the computation time required for a particular spectrum by almost a factor of three. The initial orientations are chosen weighted by the sine of the theta coordinate for each orientation. We do this by so-called "hit-or-miss" sampling: for each starting theta we need, we generate a random integer, uniform over the range 0-k, where k is the number of points on the theta grid. We then generate another random number, this time uniform and continuous over the unit line, and compare it to the sine of the trial theta. If the random number is less than sine theta, we accept the trial value of theta; if not, we reject the

trial value, and start over again with a new trial value. It is easy to see that this procedure will in fact generate a series of accepted thetas with the probability distribution proportional to sine theta.

In order to assure us that we have not made some mistake in our selection process, we run a chi-square test on the distribution of starting orientations. For a discussion of this test, and its applicability, see, for example, Rao (21, theory) or Bennet and Franklin (22, practice).

We now have completed the development of the algorithm we will use to simulate nitroxide spectra for varying degrees of motion. In the next section we will discuss the computer programs that were written to apply this algorithm, and in the last section we will discuss the results of our calculation.

IV. The Computer Program

We will now describe in some detail the actual programs that were used to implement all the calculations described above. The program was written as a series of subroutines, some of them in FORTRAN IV language, and some of them in MAP assembly language, and were designed to be run on an IBM 7090 computer under the control of the IBJOB monitor system. Most of the program is independent of the particular machine it is run on; however, those sections of the program which prepare the commands for the CalComp plotter, which actually draws the theoretical spectra, use some system subroutines peculiar to the Stanford University Computation Center. These are, however, combined into a single subroutine which may readily be rewritten for use with any other plotting machine and system.

The program was written to be as flexible as possible, and handles eight distinct, although interrelated, job types. These job types may be stacked, and each has its own form of data, preceded by a control card identifying the job type. Two of the job types are used primarily for debugging purposes, one for the solution to the hamiltonian, three for the Monte Carlo calculations, and two for replotting previously computed spectra. We will first

discuss the subroutines that are common to most or all of the various job types, and then discuss the job types themselves.

A. Common Programs

The first of the common programs we will discuss is the master control program, MASTNO. This program is quite simple: it reads in the control card preceding the data for each of the job types, and branches to the appropriate set of subroutines. For the Monte Carlo calculations, it also reads in the two parameters defining the calculation. These are STARTS, which give the number of initial orientations for the calculations, and STEPS, which give the number of jumps made by each of the simulated molecules in its "lifetime." The master program also writes the first part of a heading on the output tape, giving the job type and run date.

Common to all of the job types which generate spectra is a subroutine called PLOTNO. Spectra are generated by the simulation routines as stick spectra, that is, spectra with infinitely sharp lines whose height is proportional to the total intensity at that point. These stick spectra are generated on a grid 6000 points covering a total spectral "scan" of 150 gauss. The center of the scan is at the resonance frequency of a free electron with g-factor equal to one-third of the trace of the g-tensor.

This stick plot is written onto a scratch unit (which should be disk storage; tape read and write takes too long) to be read back in in blocks of 460 points. The plotting routine then rewinds this scratch unit, and reads in the linewidth and scale parameters to be used for the plot of the theoretical spectrum. Each point of the stick spectrum is expanded as the first derivative of a gaussian line with the input linewidth, and added to final spectrum, after being converted to the appropriate scale. When all of the points of the stick spectrum have been expanded in this way, the spectrum is normalized to have a total vertical width of ten inches, a heading is written at the beginning of the plot, a scale is drawn on the plot, and the spectrum is written out point by point. The writing of the heading and plot is done by means of a package of plotting routines in the Stanford computation center program library, and is done onto tape as a series of commands to a CalComp plotter, which then performs the actual plotting off-line. Control is then passed back to the calling subroutine.

The last of the common routines is called HEADNO and is used to complete the heading of the output tape started by MASTNO. The parameters for the hamiltonian, the Monte Carlo parameters, and size used for the grid on the surface of the θ, φ sphere are included in this heading.

B. The Hamiltonian Routine

This routine is a prerequisite to all other calculations. It reads in the parameters of the hamiltonian, specifically, the hyperfine tensor in pseudo-vector form, the $\underline{\underline{g}}$ tensor in the coordinate system in which the hyperfine tensor is reduced to a pseudo-vector, and the applied magnetic field. The program then reads in the size of the grid on the θ, φ unit sphere, and prepares tables of sines and cosines for the points of this grid. The program also reads in three control parameters, one describing the hamiltonian to be used, that is, whether the hamiltonian is to be diagonalized exactly or the approximation of section II B is to be made, the second describing the amount of output to be generated, and the third telling the program whether or not the results are to be saved on a separate output tape. In addition, a 72-character title which is then used as a heading for all output generated from this hamiltonian is read in.

The program proceeds in one of two ways, depending on which solution of the hamiltonian is required.

If the exact solution is required, for each point on the grid, the magnetic field in the molecular coordinate system, and the effective electron field, $\underline{H}_e$, is computed. Matrices for the three components of the nuclear spin vector and the electron spin vector are dotted into the

external and effective electron magnetic fields, multiplied by the appropriate factors, and added to the hamiltonian matrix. The hyperfine pseudo-vector is dotted into the three components of the SI pseudo-vector, and added to the hamiltonian matrix. The hamiltonian matrix is generated as a 12x12 real symmetric matrix as in equations 2.6 and 2.7, and is then diagonalized by a subroutine adapted from SHARE. From the exact eigenvalues and eigenvectors of the hamiltonian, the transition frequencies and intensities are computed, and these are then added to the stick spectrum of a powder sample being generated. After all the points on the grid have been covered, the stick spectrum is plotted by PLOTNO and control is returned to MASTNO.

If the approximation of section II B is to be made, after computing the external and effective electron magnetic fields at each point, the two effective nuclear fields are generated. From their magnitudes, the transition frequencies are computed. Their dot product is taken, and from this the matrix of overlap integrals is formed, and is used directly as the relative transition moments. These moments and frequencies are treated as for the exact moments and frequencies.

C. Monte Carlo Calculations

There are three job types that are concerned with Monte Carlo calculations. As is usual in such calculations, accuracy is sacrificed for speed. All of the numerical work is done from tables which have been previously prepared. For our work, we use five-bit accuracy for most of the tables (tables of transition frequencies, which are not used for any arithmetic, are kept to higher accuracy).

The first of the three job types is designed to prepare these tables on a tape, to be read in and used at some future date. Of course, the tables are left in core after preparation, and the program assumes one particular Monte Carlo calculation will be performed immediately.

The Monte Carlo routines assume that a run of the hamiltonian solution routines has been previously made and the transition frequencies and moments from that run have been saved on a tape. These frequencies are then read in, and the frequencies of the three strong transitions are converted to index positions for a stick spectrum. The program assumes that a mesh of 32 points was used for each angle. This is done so that we may index the theta and phi coordinates in separate index registers and then take the logical "or" of these registers to get the true index position. If the mesh size was not a power of two, this could not be done directly, and would cause a large increase in running time for the Monte Carlo program. If the mesh

size used in the calculation was not 32, the program writes an error message on the output tape and terminates execution.

A table of five-bit sines is prepared. A table giving the relative probabilities of increasing and decreasing theta is also prepared, and converted to five-bit accuracy. These tables are then written out onto a tape, and the program proceeds to the first Monte Carlo calculation, using the values of STARTS and STEPS read into core storage by the master program.

For each of the required initial orientations, a random number is generated by the multiplicative-congruence method described above. The first five bits of this number are used for the starting value of phi. (In general, higher order bits tend to be more random than lower order bits in a number generated by this method. We never use more than the first ten bits of the 35-bit random number.) We then generate a second random number and use the leading five bits of it as a trial value for the initial value of theta. The second five bits of this random number are compared to the entry in the five-bit sine table corresponding to the trial value of theta; if the random number is less than or equal to the entry in the table, the trial value is accepted. If not, the trial value is rejected, and we begin again with a new random number. When we have found an acceptable theta and phi, we add one to the value of phi, shift it five bits

to the left, and place it in index register A; the theta value is placed directly in index register B. Whenever we wish to find an entry in our frequency tables corresponding to the values of theta and phi in these index registers, we simply form the logical "or" of the two registers and use the result as an index position in the vector array of frequencies. Needless to say, the frequency tables were prepared by the same indexing procedure. This procedure is quite efficient, in that one need not waste any positions in core storage for unindexible frequencies, as we would if we did not use a power of two for the grid size, and in that the logical "or" is taken directly by the machine, using multiple tagging of index registers, and does not cost any more computer time than a single indexing procedure.

Having determined the starting coordinates in orientation space, we now allow the molecule to jump. If no jumps are required, that is, if we want to generate a powder spectrum by the Monte Carlo method, we take the frequencies corresponding to the initial orientation coordinates and add them to a stick spectrum, much in the same way we form the stick spectrum for a true powder sample.

If we are doing a Monte Carlo motional calculation, for each of the jumps the molecule is scheduled to take, we generate a random number. If the first bit of the random number is a one, we make the jump in the phi

direction; if a zero, in the theta direction. If we are jumping in phi, the next bit of the random number is used to determine whether we increase or decrease it. If we are jumping in theta, we compare the next five bits of the random number to our table of relative probabilities for increasing or decreasing theta. If it is less than or equal to the entry in the table corresponding to the present theta coordinate, we decrease theta; if greater, we increase theta. We add the frequencies corresponding to the new coordinates to our average, and continue to the next jump.

We have mentioned earlier that we need only develop our grid on the half-sphere, since we may obtain the frequencies for the other half-sphere by (inversion) symmetry. If a jump is taken in theta, whose range is zero to pi, we have no problem, for the relative probabilities are such that there is zero probability of jumping past a pole. However, if a jump is taken in phi, which also ranges from zero to pi, we must consider the effects of jumping past the boundaries of our tables. After each jump in phi, we test to see that we are still within the half-sphere whose frequencies are tabulated, and if we find we are not, we add or subtract pi from the phi coordinate (depending on which endpoint we have jumped past), and subtract the theta coordinate from pi to get the mirror image position of the new coordinate, which is within the tabulated range.

After we have completed all of the required jumps, we divide the sum of transition frequencies sampled in the random walk by the number of orientations sampled, STEPS + 1, and add these averaged frequencies onto the stick spectrum. At present, there is an upper bound of 32,767 to the number of jumps that a given molecule can take. This number is determined by the size of the register used to contain the number of jumps still to be taken; the programs may be modified to extend this range, but we have not found it necessary.

When we have simulated a random walk of the required number of steps for all of the molecules specified by STARTS, we call the subroutine PLOTNO to plot the resultant theoretical spectrum, after which we return control to MASTNO.

The other two job types used for Monte Carlo simulation are different from the above, only in that they assume different locations for the tables used in the random walk simulation. While the job type described above prepares the tables from the tape of frequency-moment calculations generated directly by the solution to the hamiltonian, one of the remaining two jobs assumes these tables are left in core, and the other assumes the tables themselves have been written onto a tape, and reads them in from this tape. Both of these job types then proceed as above.

D. Replotting Routines

Two of the job types that the program can handle are designed to replot a previously generated spectrum. One of these two starts with a tape of transition frequencies and moments, as generated by a run of the hamiltonian-solution routines, and plots a powder spectrum from this tape. Plotting is done exactly as it is done by the original program generating the tape.

The second of the replotting routines is used to vary the linewidth and scale parameters used for a plot done previously, whose stick spectrum is still left on the scratch unit by the plot routine. This subroutine was used to decide the appropriate linewidth parameter for a series of Monte Carlo calculations.

E. Debugging Routines

There are two routines in the complete package that are used primarily for debugging purposes. One of these is a routine to reset the starting value of the random number generator. It is used to redo a particular calculation with the same sequence of random numbers as used before. A comparison of the results of the two calculations affords a check on program modifications.

The second routine is one that is used to perform statistical tests on the sequence of orientations generated

in a particular Monte Carlo calculation. If requested, a Monte Carlo run will generate a tape containing the initial coordinates and frequencies and the final coordinates and averaged frequencies for the run. These are then used in a chi-square test for randomness in the distribution of orientations. Provision has been made to check the correlation between initial and final orientations, but the test would be valid only for a run with a very large value of STARTS. Unfortunately, the grants of computer time made to the author were not sufficient to make such a long run (of the order of a few hours of machine time), so that these tests were never run. A crude check for bias in the jumping is afforded by the spectrum in the complete averaging limit. If this spectrum has the splitting of the three hyperfine lines equal to the solution splitting, we know that our bias cannot be very large. In fact, solution spectra generated by the Monte Carlo calculation do have the appropriate splittings so that we are confident that our jumping procedure is free from bias.

The description of the programs given above is purposefully short. Additional information and program listings are available from the author, along with copies of the program decks and information about data formatting, etc.

We now proceed, in the next section, to describe the results obtained with our programs, and compare these results with experimental spectra.

V. Results and Conclusions

In the three preceding sections we have discussed the various methods we will use to simulate nitroxide radical EPR spectra. We will now exhibit the results of such simulation and compare them with the experimental spectra. For convenience, the structural formulae of all the compounds under discussion are reproduced as figure 5.1.

A. Spectra in the Absence of Molecular Motion

In an attempt to determine the region of validity of the approximation of section II B, we chose the radical-ion chlorpromazine, VIII, at Q-band for our first calculation. Although this radical is not really a nitroxide, its hamiltonian may be represented as in equation 2.2. The radical is unstable, and it has not been obtained as a fully oriented sample. Principal axis splittings have been determined, however, from the spectra of flowing solutions of chlorpromazine attached to deoxyribonucleic acid (DNA). It is presumed that the radicals are attached to the DNA molecules in fixed orientation, and that the shear forces in the flowing solution are sufficient to orient the DNA, and, therefore, the chlorpromazine. The spectra are well

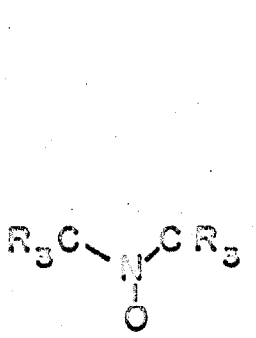

I

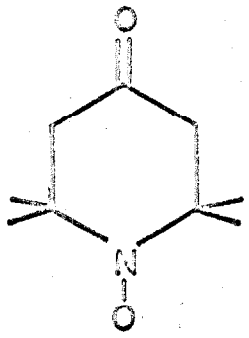

II

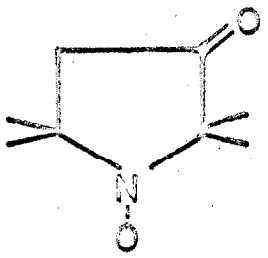

III

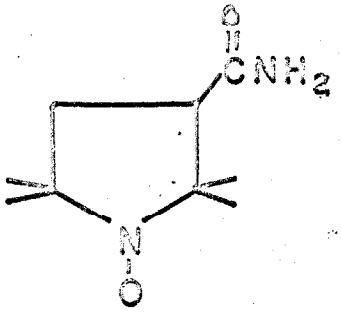

IV

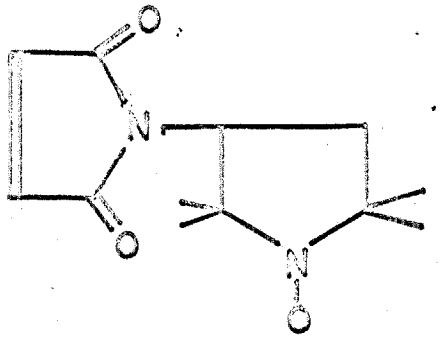

V (Maleimide Reagent)

Fig. 5.1. Structures of the various compounds under discussion

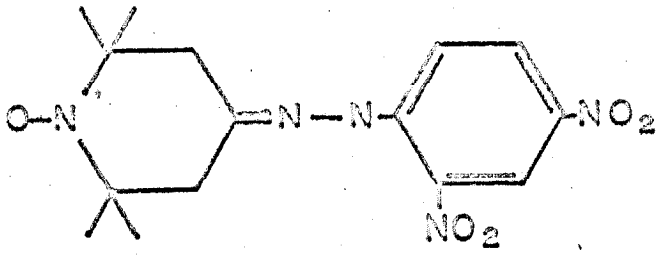

VI (Hapten Nitroxide)

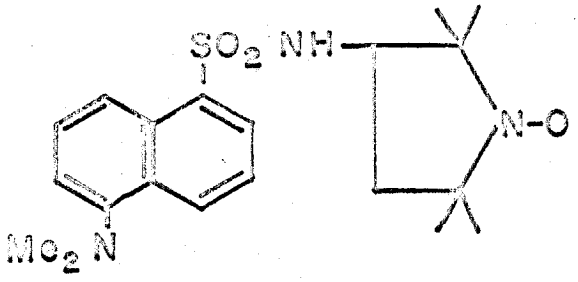

VII (Dansyl Nitroxide)

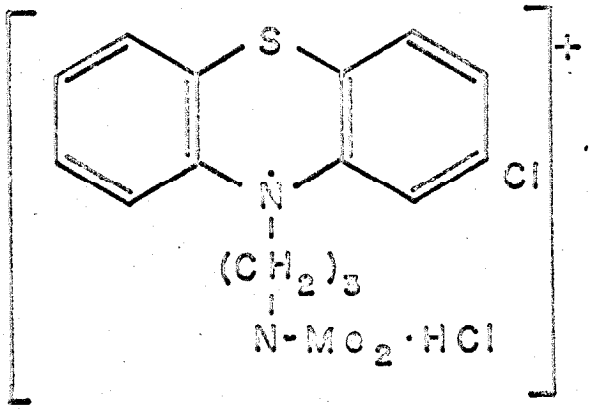

VIII (Chlorpromazine Radical-ion)

Fig. 5.1. (continued)

resolved only when the flow is parallel to the applied magnetic field; from the spectra in this case, we may determine the largest principal axis splitting, and from the value of the solution splitting, we may determine the mean perpendicular splitting. Under the assumption of axial symmetry, we obtain for the hyperfine pseudo-vector, $\underline{\mathcal{T}}$:

$$\underline{\mathcal{T}}^{t} = (7.3, 7.3, 44.6) \tag{5.1}$$

It is difficult to measure the $\underline{g}$ tensor from these spectra. The original estimate in the paper of Ohnishi and McConnell (1) is:

$$\underline{\underline{g}} = \begin{pmatrix} 2.003 & 0 & 0 \\ 0 & 2.003 & 0 \\ 0 & 0 & 2.006 \end{pmatrix} \tag{5.2}$$

The applied magnetic field is 12400 G.

In figure 5.2(a) the experimental powder spectrum of the radical attached to DNA is shown. In figure 5.2(b) the theoretical spectrum generated with an assumed line-width of 8.0 gauss and the parameters above is shown. In figure 5.2(c) we show the spectrum obtained when the hyper-fine pseudo-vector is taken as above and the anisotropy in the $\underline{g}$ tensor is taken as:

$$\underline{\underline{g}} = \begin{pmatrix} 2.002 & 0 & 0 \\ 0 & 2.002 & 0 \\ 0 & 0 & 2.006 \end{pmatrix} \tag{5.3}$$

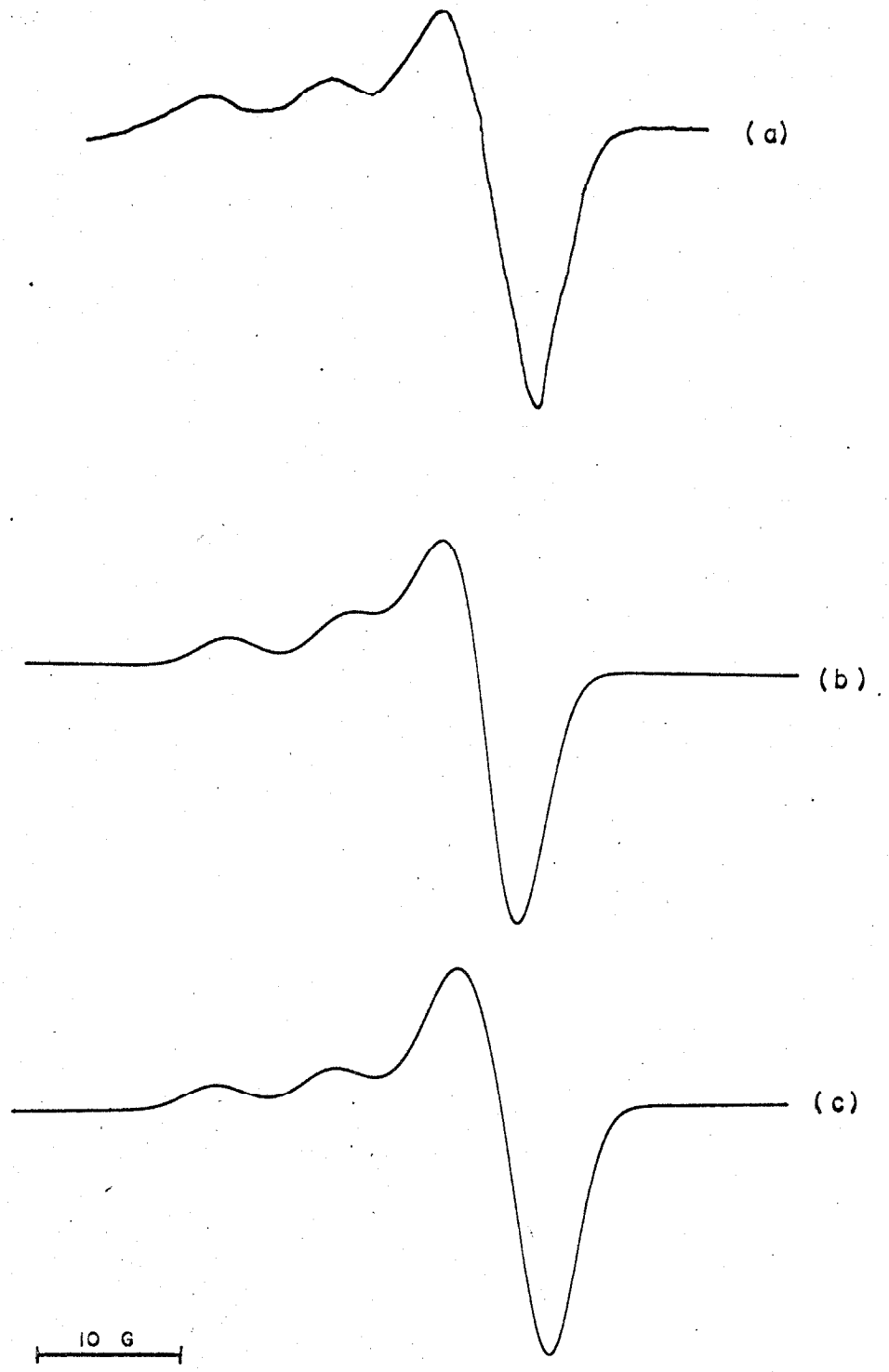

Fig. 5.2. Spectra of chlorpromazine radical-ion
(a) Experiment
(b) Theory $\Delta g = 0.003$
(c) Theory $\Delta g = 0.004$

Both of the theoretical spectra exhibited are calculated using the approximation of section II B. A calculation using exact solutions to the hamiltonian gave a spectrum exactly superimposable on the approximate spectra. The experimental spectrum and parameters are taken from the work of Ohnishi and McConnell (1).

For the following reasons we believe that the above spectrum provides a sensitive test of the approximation. For some orientations of the field, the nuclear Zeeman and hyperfine fields are approximately equal in magnitude and oppositely directed. Whenever this occurs, as discussed above, we expect the approximation to fail. Indeed, the forbidden transitions for these orientations become about 20 per cent as intense as the allowed transitions, and single orientation spectra calculated by the two methods are barely similar. However, the resultant powder spectra are identical, and therefore we assert that our approximation is valid for chlorpromazine radical-ion powder spectra. For typical nitroxides at X-band, the nuclear Zeeman term is reduced by a factor of about four, and the hyperfine term is increased by about a factor of three. There are now no orientations where cancellation of the two contributions occurs, and, a fortiori, the approximation is valid.

We next studied the spectra of compound IV, an amide nitroxide. Accurate single crystal solid solution

work has been done on this compound, and the hyperfine pseudo-vector and $\underline{\underline{g}}$ tensor are experimentally determined; their values are given below:

$$\underline{T}^{+} = (14.0,\ 14.0,\ 87.0)$$

$$\underline{\underline{g}} = \begin{pmatrix} 2.0089 & 0 & 0 \\ 0 & 2.0061 & 0 \\ 0 & 0 & 2.0027 \end{pmatrix} \qquad (5.4)$$

The residual linewidth in single crystal is about four gauss. We found that we need take a value of about five gauss in order to fit the experimental powder spectrum. It is not hard to see that this increase is probably attributable to dipolar contributions, which one would expect to be more important in an unoriented sample, since some of the magnetic neighbors of a given radical are expected to be closer here than in single crystal. (The term powder spectrum is here used to signify any unoriented sample; experimentally the spectra are usually taken in solution in a glass at liquid nitrogen temperatures.) We here have no leeway in the choice of parameters. Using the values cited above, we calculate the powder spectrum shown in figure 5.3(b);* an experimental powder spectrum, kindly taken by S. Ohnishi, is shown in figure 5.3(a).

---

*Exact spectra are superimposable on the approximate spectra; we used the approximate hamiltonian.

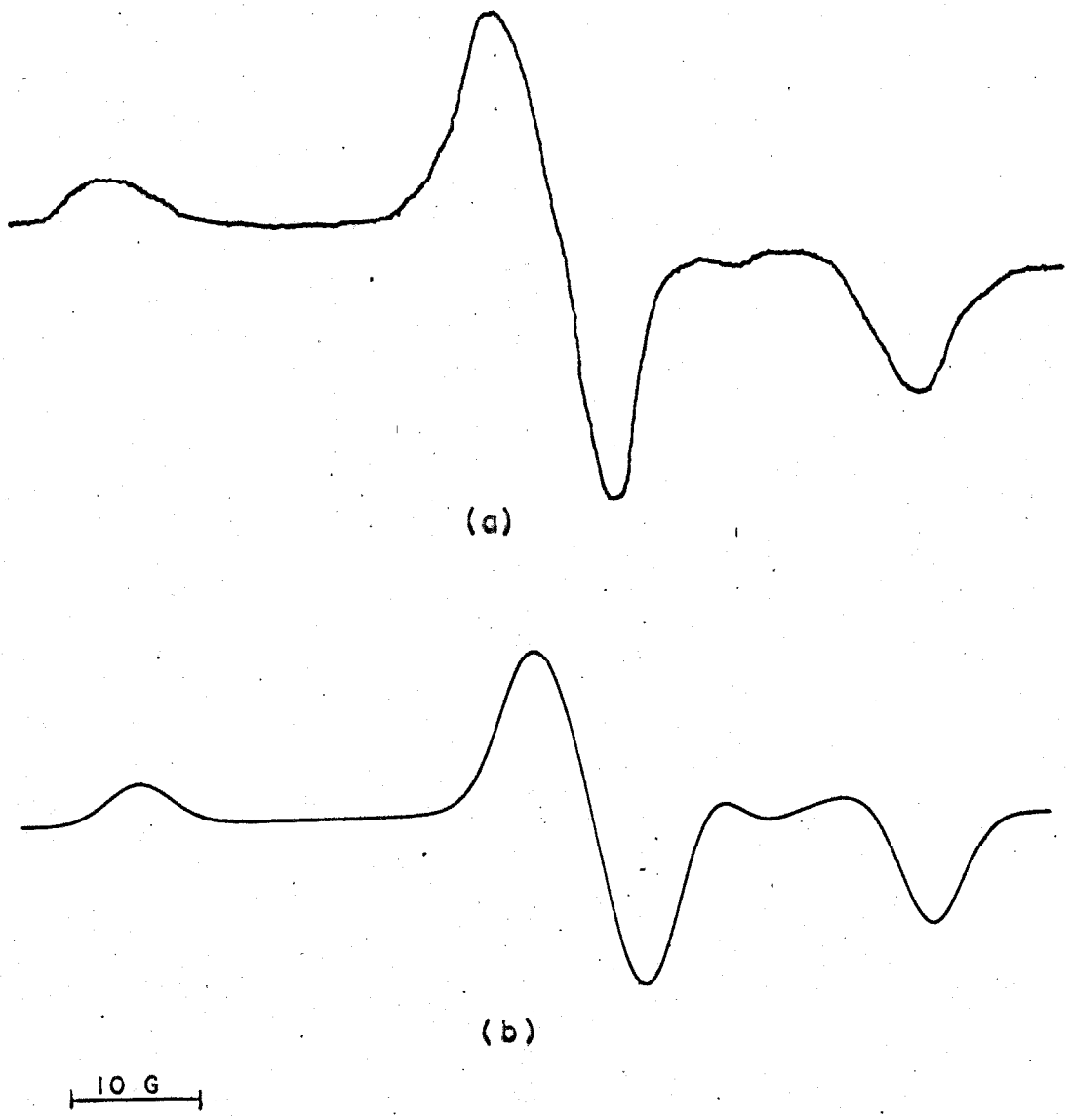

Fig. 5.3. Spectra of nitroxide IV
(a) Experiment
(b) Theory

One more radical was studied in the absence of motion, the radical of spin-labeled haemoglobin. In this radical neither the $\underline{g}$ nor the hyperfine tensors are axially symmetric. Single crystal spectra calculated by the approximation of section II B agree with the experimental spectra.

B. Spectra in the Presence of Motion of the Spins

For all of the Monte Carlo calculations we performed, the hamiltonian parameters were taken to be those of radical IV. Unfortunately, the experimental work was not done on this radical, but on dansyl nitroxide, VII, whose hamiltonian parameters have not been measured. We hope that the parameters for these two compounds are not very different.

We first attempted to provide a check on the Monte Carlo method for choosing molecules with random orientations, and to estimate the number of single molecules required to obtain convergence to the true spectrum. We ran a series of Monte Carlo calculations using 100, 1000, and 10000 randomly chosen orientations, and obtained the spectra shown in figures 5.4 (a), (b), and (c), respectively. It is observed that the spectra for 1000 and 10000 orientations are quite similar to each other and to the experimental powder spectrum. It is obvious that the more averaging, that is, the more motion present in a sample, the fewer

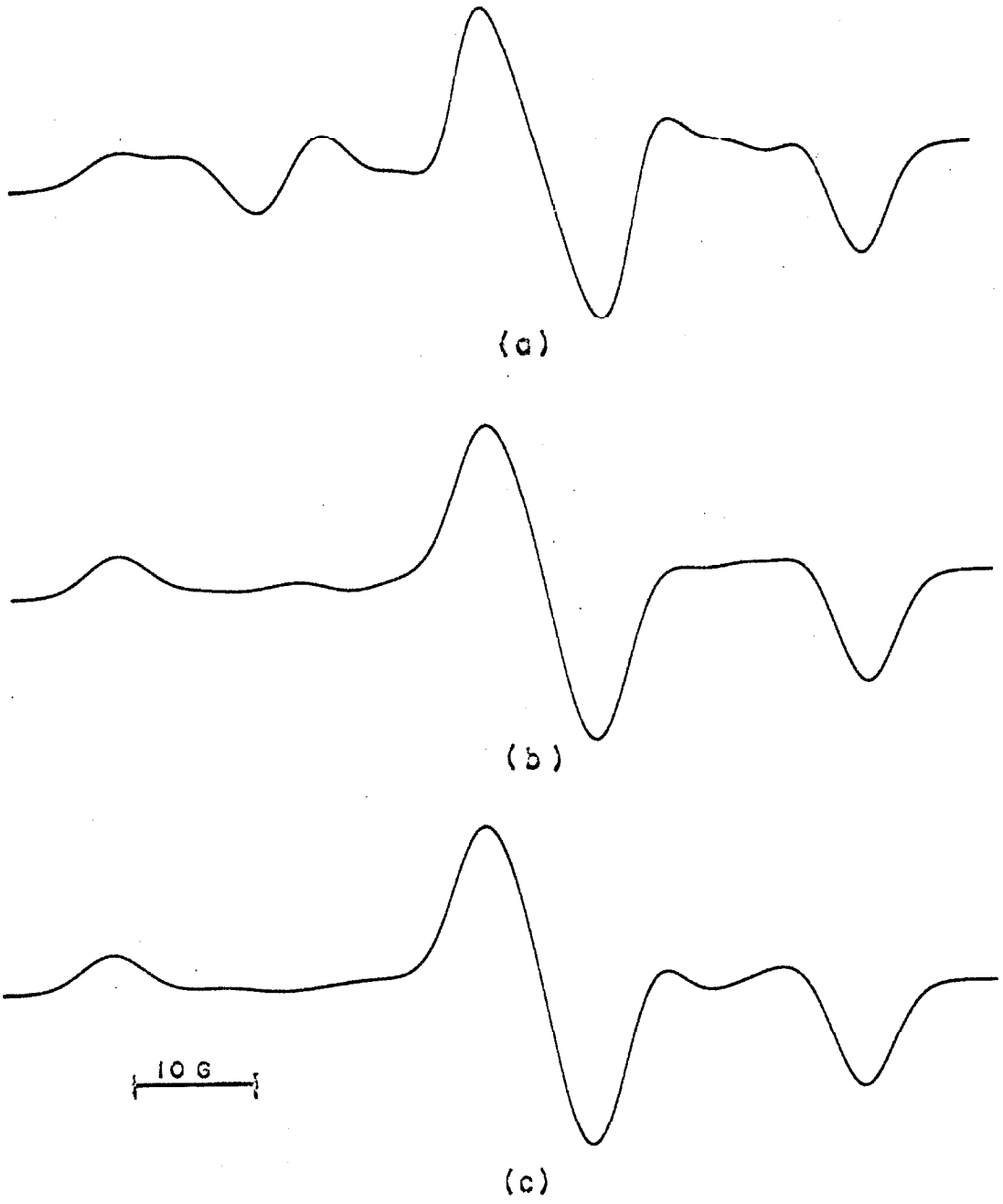

Fig. 5.4. Monte Carlo powder spectra
(a) 100 orientations
(b) 1000 orientations
(c) 10000 orientations

initial orientations are needed to obtain convergence. Computation time is linear in the number of starting orientations; we therefore chose 1000 as the canonical number and used it for all of the spectra in the presence of molecular motion.

In order to reassure ourselves that our random number generator was in fact generating random numbers, and that our selection process was unbiased, we ran a chi-square test on the theta and phi distributions in initial orientations for a sample of 1000. Although the number of possible values for theta and phi is 32 for both, the expected populations for those states with theta near the poles are small, and, in accordance with standard practice, were not considered in the test. We obtained the following values for chi-square:

$$\begin{aligned} \chi^2_{\varphi}(31) &= 34.75 \\ \chi^2_{\theta}(28) &= 28.24 \end{aligned} \qquad (5.5)$$

The numbers in parentheses on the left side of the equations are the degrees of freedom for each variable. These values are well within the 5 per cent confidence levels for the appropriate number of degrees of freedom. Of course this test merely serves to eliminate errors of the first kind, where we reject the hypothesis that the numbers are randomly chosen from the assumed distribution, when they are so chosen; a more sensitive test would

eliminate errors of the second kind, where we accept the hypothesis even though it is false. The method used for such a test is, in general, dependent on the type of bias of which one is most afraid, and is exceedingly difficult to apply. We are content with our cruder test, and the additional confirmation of having obtained the right answer.

Having decided that our Monte Carlo routine was debugged, we proceeded to allow motion of the spins. Presumably, we would want to run statistical tests on the random jumping procedure, as discussed in section IV E, but we could not afford the expense of such a run.

We chose four different values of solution viscosity, by coincidence those very same values reported by Stryer and Griffith (3), which give qualitatively different spectra for our motional problem. The four experimental spectra were taken of solutions of dansyl nitroxide in 95% water-5% ethanol, 76% glycerol-19% water-5% ethanol, both at 23°C, 90% glycerol-5% water-5% ethanol at 35°C, and -15°C; the experimental spectra, taken from (3), are shown as the upper spectra of figures 5.5-5.8.

We computed theoretical spectra for the radical IV for a large series of jumps for each molecule, ranging from one jump to 20000. A run of 1000 initial configurations and 20000 jumps/molecule requires about 35 minutes of IBM 7090 computer time. We believe that 20000 jumps are sufficient to

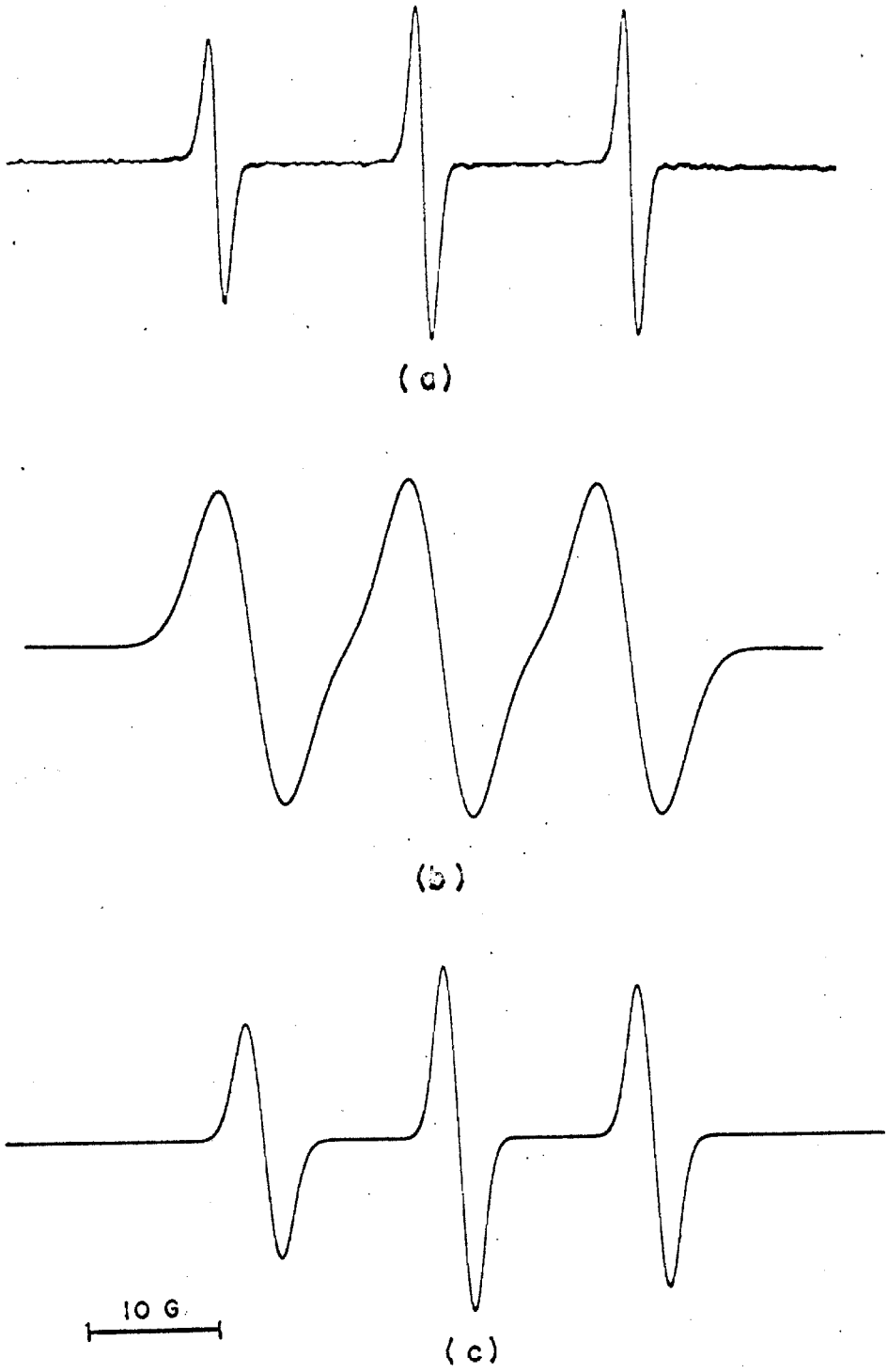

Fig. 5.5. (a) Dansyl nitroxide in 95% water-5% ethanol at 23°C
(b) Monte Carlo calculation: 20000 jumps, 5 gauss linewidth
(c) Same, 2 gauss linewidth

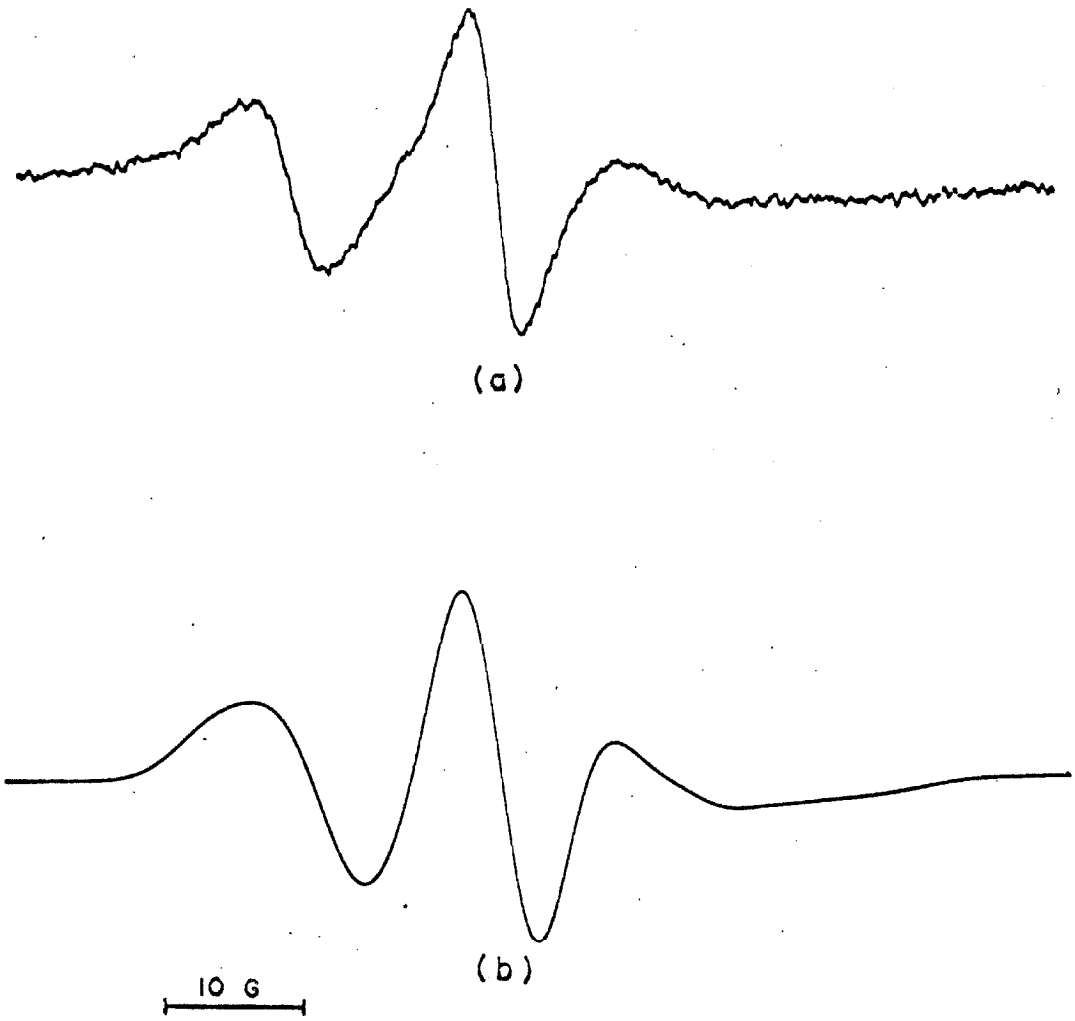

Fig. 5.6. (a) Dansyl nitroxide in 76% glycerol-19% water-5% ethanol at 23°C
(b) Monte Carlo calculation: 250 jumps

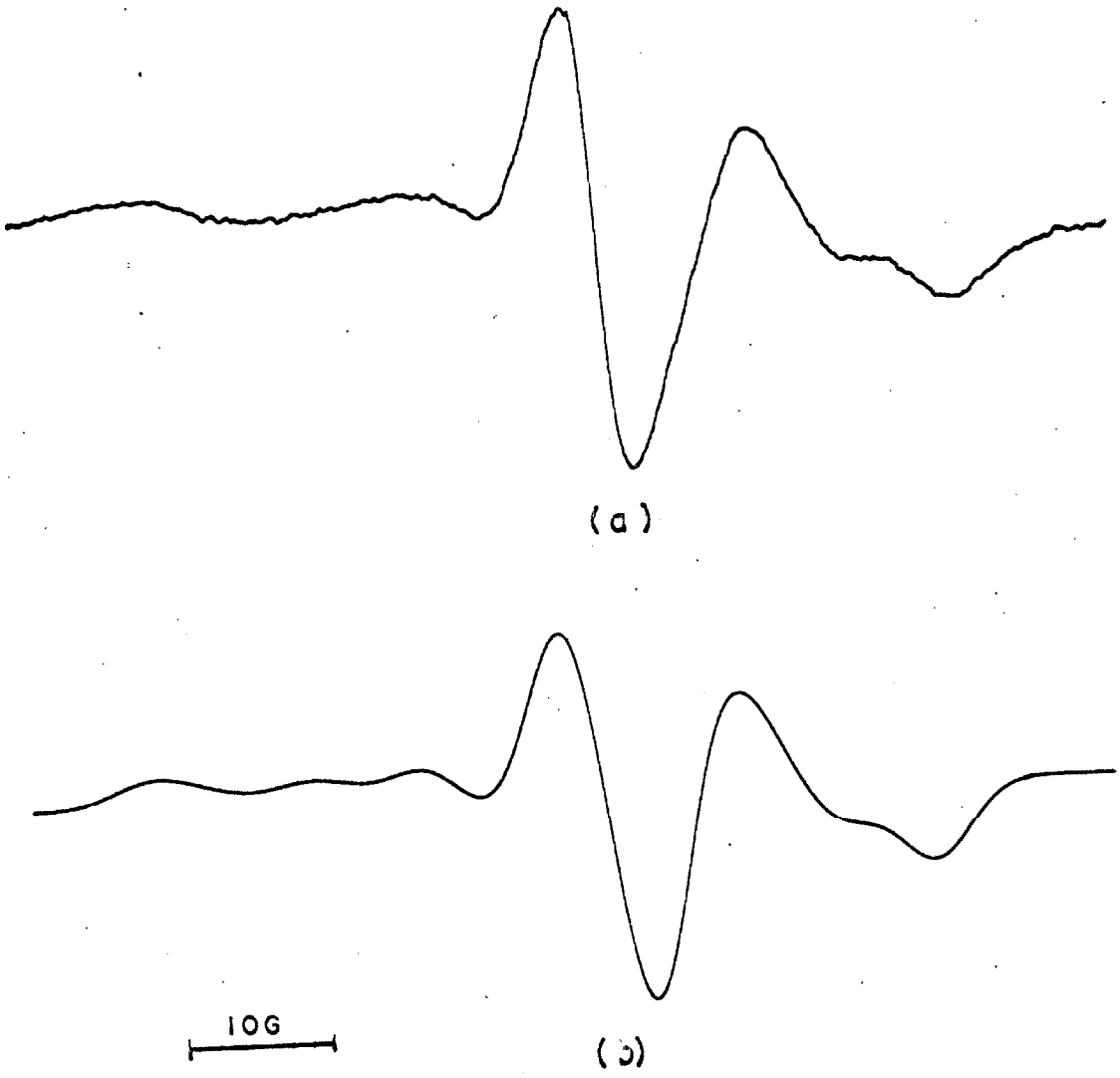

Fig. 5.7. (a) Dansyl nitroxide in 90% glycerol-5% water-5% ethanol at 35°C
(b) Monte Carlo calculation: 100 jumps

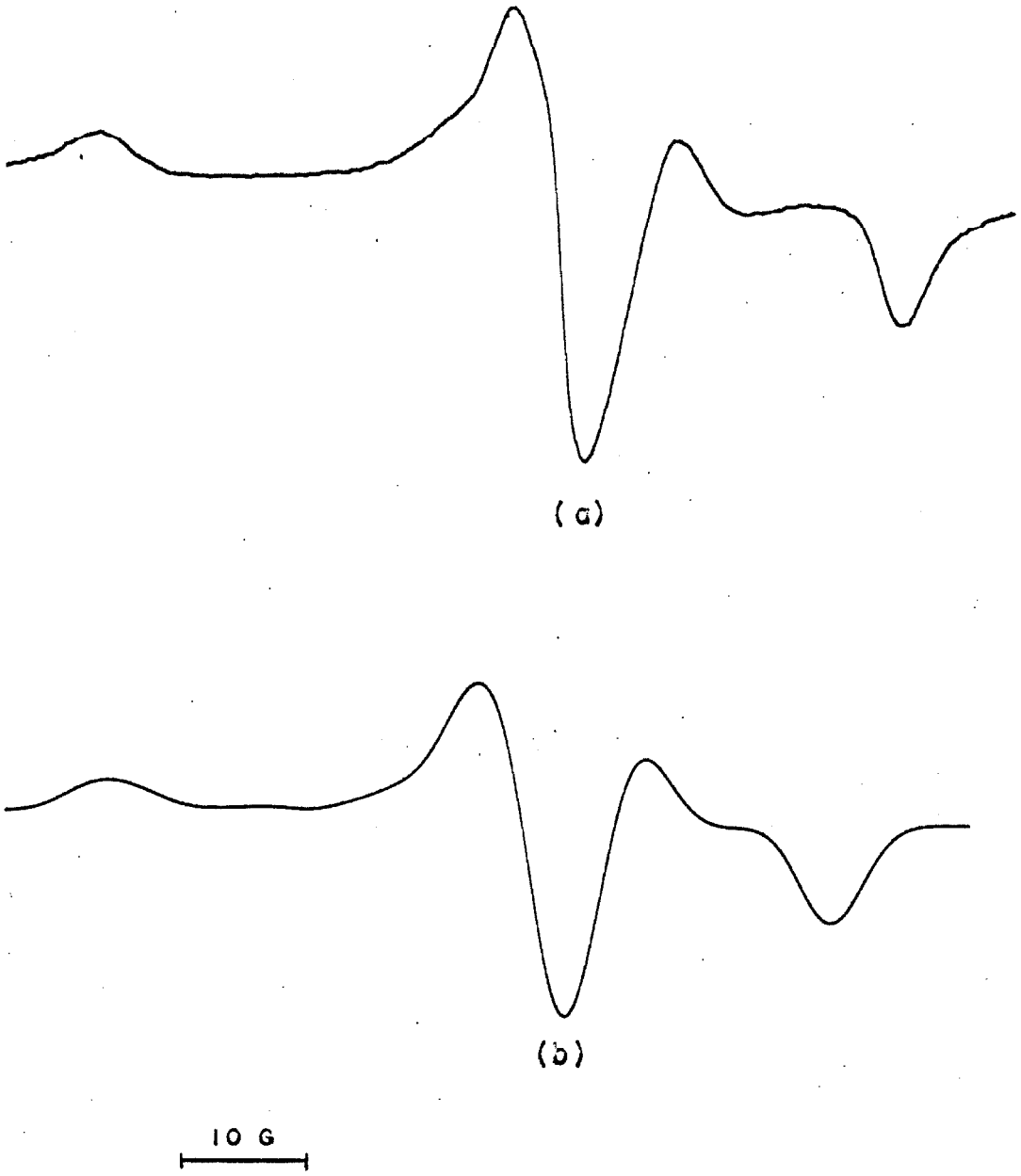

Fig. 5.8. (a) Dansyl nitroxide in 90% glycerol-5% water-5% ethanol at -15°C
(b) Monte Carlo calculation: 50 jumps

average out almost all of the anisotropic interactions. We are somewhat belied by the unequal linewidths for the three hyperfine components of the spectrum, but we observe that the experimental spectrum of the radical IV in water at 25°C also shows this asymmetry. Presumably if we allowed the molecule to take many more jumps in its lifetime, we would expect this variation of linewidth to disappear. With the current version of the computer programs, we can only increase the jumping rate by a factor of 1.6, which is not sufficient to complete the averaging. Again computer costs for further averaging become prohibitive, certainly compared to the additional information obtained.

We matched the experimental spectrum shown in figure 5.5 (a) by allowing the molecule to take 20000 jumps in its effective lifetime; the theoretical spectrum so obtained is shown in figure 5.5 (b). The other experimental spectra were fit as follows:

Experimental spectrum	Jumps/ molecule	Theoretical spectrum
5.5(a)	20000	5.5(b)(c)
5.6(a)	250	5.6(b)
5.7(a)	100	5.7(b)
5.8(a)	50	5.8(b)

In each case, the spectrum labeled (b) was plotted with a linewidth parameter of five gauss; the last three theoretical spectra are seen to be in very good agreement with the

experimental spectra. The first of this group of spectra, taken in almost freely rotating solution, does not fit with a linewidth of five gauss. Figure 5.5 (c) shows the same spectrum replotted with a linewidth of two gauss, and is in fairly good agreement with the experimental spectrum. This additional narrowing in nonviscous solution may be attributed to the averaging out of anisotropic contributions to the residual proton hyperfine interaction. Part of the lack of agreement may be attributed to the fact that the compound used for the experimental spectrum probably does not have exactly the same hamiltonian parameters as compound IV, which was used for the theoretical study; in fact, the isotropic part of the hyperfine interaction is different for the two compounds as evidenced by the different splitting in freely rotating solution. The excellent agreement between the theoretical and experimental spectra precludes a very large difference between the two sets of parameters.

We are able to obtain an estimate of the rotational correlation time, ρ , from our work. The rotational correlation time may be defined as the time in which a molecule has forgotten where it started. More precisely, we form the statistical average over molecules of the product of an orientation parameter at time t=0 and the same parameter at time t=T; if we assume this function to be an exponential

then the inverse of the rotational correlation time is the logarithmic derivative of the function with respect to T. Since we are working with an orientation parameter that may be characterized as a scalar index number (in particular, we may use the grid-indexing procedure as described in section IV C), we may define a correlation time as that time in which the molecule has moved from its initial index position to one m spaces removed. The number of jumps required to move m spaces away from the starting position is proportional to m^2; we may then write for the ratio of the rotational correlation time to the molecular lifetime:

$$\frac{\rho}{\Delta t} = \frac{m^2}{N} \tag{5.6}$$

where N is the number of jumps taken in a lifetime. Inserting the minimum lifetime of the inverse of the hyperfine frequency, and a value of m=16 (giving an angular motion of $\pi/2$ radians) we obtain as a lower bound for the rotational correlation time of the system having EPR spectrum shown in figure 5.7 a value of 50 nanoseconds. Stryer and Griffith (3) obtain a value of 36 ns. by fluorescence depolarization measurements. Krause and O'Konski (23) obtain a value of 200 ns. by electric birefringence measurements on γ-globulin. The accuracy of the fluorescence depolarization method is not known.

C. Summary and Conclusions

We have seen that a spin hamiltonian for nitroxide or similar radicals may be written. We have presented both the exact and approximate solutions to this hamiltonian, and shown that, for the region of experimental interest, the approximation is sufficiently accurate to enable us to fit all of the polycrystalline spectra that have been obtained experimentally. We have examined the effect of molecular motion on the spectrum, and shown that the EPR experiment introduces an effective lifetime into the system, and that we may treat the motion of the molecule in times short compared to this lifetime semi-classically. If we average the values of transition frequency that a molecule samples in a time of the order of its lifetime, we obtain spectra which are in excellent agreement with experiment. We have performed Monte Carlo calculations on a variety of different radicals and their environments, and fit all of the corresponding spectra.

We conclude that the approximation scheme developed above for the motion of these radicals in solution is sufficiently accurate to account for the known experimental results.

We also claim that this method may be of somewhat greater generality than we have hitherto asserted. It may presumably be used for calculations on any system, the

position of whose electric dipole transitions is a function of orientation. The experiment to determine the spectrum will introduce a characteristic minimum lifetime into the system, of the order of the inverse of the separation between transitions, and we may use the above-described Monte Carlo method to average frequencies over the motion that takes place in this characteristic lifetime.

References

1. S. Ohnishi and H. M. McConnell, J.A.C.S., 87, 2293 (1965).

2. T. J. Stone, T. Buckman, P. L. Nordio and H. M. McConnell, P.N.A.S., 54, 1010 (1965).

3. L. Stryer and O. H. Griffith, P.N.A.S., 54, 1785 (1965).

4. O. H. Griffith and H. M. McConnell, P.N.A.S., 55, 8 (1966).

5. L. J. Berliner and H. M. McConnell, P.N.A.S., 55, 708 (1966).

6. S. Ohnishi, J. Boeyens and H. M. McConnell, to be published.

7. E. G. Rozantzev and L. A. Krinitzkaya, Tetrahedron, 21, 491 (1965).

8. O. H. Griffith, D. W. Cornell and H. M. McConnell, J. Chem. Phys., 43, 2909 (1965).

9. D. Kivelson, J. Chem. Phys., 33, 1094 (1960).

10. a) R. Kubo and K. Tomita, J. Phys. Soc. Japan, 9, 888 (1954).

    b) R. Kubo in Fluctuation, Relaxation and Resonance in Magnetic Systems, ed. D. Ter Haar (Edinburgh: Oliver and Boyd, 1962).

11. P. W. Anderson and P. R. Weiss, Rev. Mod. Phys., 25, 269 (1953).

12. P. W. Anderson, J. Phys. Soc. Japan, 9, 319 (1954).

13. I am indebted to Mr. Lyle Smith of the Stanford University Computation Center for pointing this theorem out to me.

14. See, for example, E. Bodewig, Matrix Algebra (New York: Interscience), pp. 158 ff.

15. N. Bloembergen, E. M. Purcell and R. V. Pound, Phys. Rev., 73, 679 (1948).

16. a) J. H. Van Vleck, Phys. Rev., 74, 1168 (1948).

b) J. H. Van Vleck and G. J. Gorter, Phys. Rev., 72, 1128 (1947).

17. J. M. Hammersley and D. C. Handscomb, Monte Carlo Methods (New York: Wiley, 1964).

18. Yu. A. Shreider, Method of Statistical Testing (New York: Elsevier, 1964).

19. J. Von Neumann, Monte Carlo Method, N.B.S. Appl. Math Series, 12, 36 (1951).

20. A good review article on random number generators is that of T. E. Hull and A. R. Dobell, SIAM Review, 4, 230 (1962).

21. C. R. Rao, Linear Statistical Inference and Its Applications (New York: Wiley, 1965).

22. C. A. Bennett and N. L. Franklin, Statistical Analysis in Chemistry and the Chemical Industry (New York: Wiley, 1954).

23. S. Krause and C. T. O'Konski, Biopolymers, 1, 503 (1963).

PROPOSITION I

The Singlet Triplet Gap in Wurster's Blue Perchlorate

Abstract

Crude a priori calculations of the singlet-triplet gap (J) and the exciton bandwidth (J') for single crystals of Wurster's Blue Perchlorate are described.

I. Introduction

One of the first solids in which triplet excitons were observed is Wurster's Blue Perchlorate (WBP) (p-N,N,N',N' tetramethyldiaminobenzene perchlorate) (1,2). Magnetic resonance measurements of the temperature dependence of the magnetic susceptibility of WBP show that the compound may be characterized by an excitation energy for triplet excitons, J, of the order of 250 cm^{-1}, and an effective exciton bandwidth, J', of the order 5 cm^{-1} (2). The crystal structure of WBP at high temperatures has been determined (3), and it has been shown that the Wurster's cations, which are shown in figure 1, lie in linear chains, as shown in figure 2. The aromatic rings of adjacent molecules lie in parallel planes separated by 3.64 Å; the

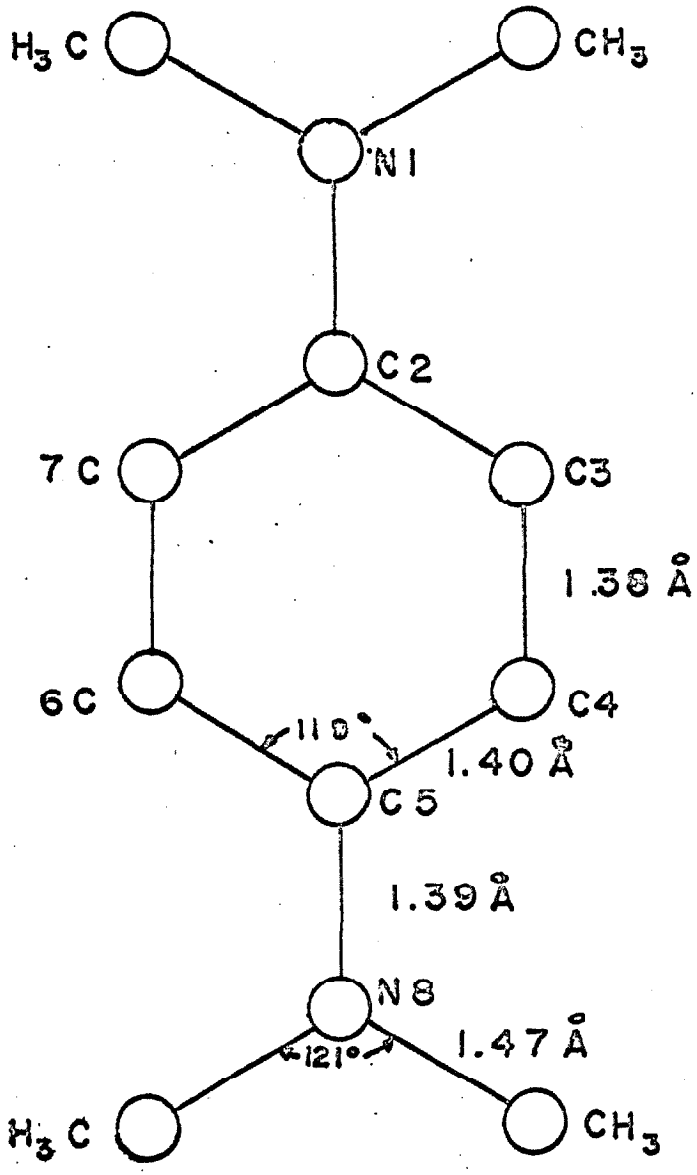

Fig. 1. Schematic diagram of a single Wurster's cation

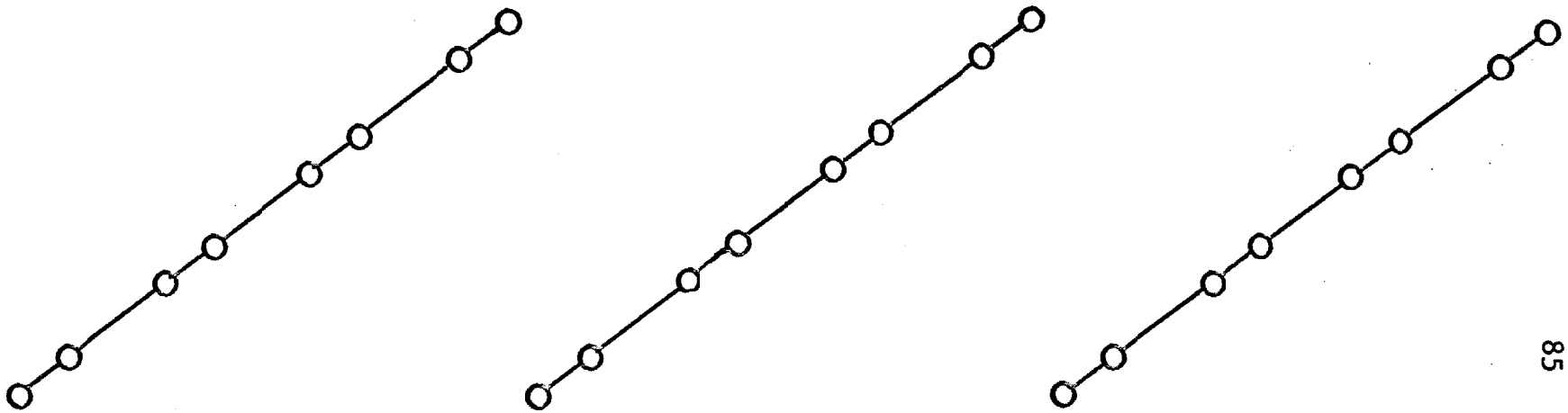

Fig. 2. Schematic diagram of a chain of Wurster's cations in WBP

closest pair of nitrogen atoms on adjacent molecules are separated by 3.74 Å. We may write the spin hamiltonian for a single chain of these molecules as:

$$\mathcal{H} = \sum_{n=0}^{N/2} \left\{ J \underline{S}_{2n}^{+} \underline{S}_{2n+1} + J' \underline{S}_{2n+1}^{+} \underline{S}_{2n+2} \right\} \qquad (1)$$

where J and J' are defined above, and $\underline{S}_{2n}$ and $\underline{S}_{2n+1}$ represent the spins on the $2n^{th}$ and $2n+1^{st}$ molecules, which together form the n^{th} site. It is well known that at 186°K there is a sudden decrease in the magnetic susceptibility of WBP, attributed to a phase change in which the cations, which act as magnetic doublets at high temperatures, pair up to form dimers with singlet ground states and triplet excited states. Preliminary work on the low-temperature crystal structure (4) has shown that there is indeed a doubling of the unit cell due to dimerization. Unfortunately no measurements of interatomic distances in the low temperature form of WBP are available. If triplet excitons may be considered to be localized, and their motion diffusional, Soos (5) has shown that if the true J' is much larger than the 5 cm^{-1} effective bandwidth, say of the order of 150 cm^{-1}, both the absence of hyperfine structure and the exchange narrowing of the exciton resonance lines may be accounted for. Thus it is evident that an a priori calculation of the magnitudes of J and J' would be of great importance in the theory of triplet excitons.

II. Theory

We will consider the evaluation of the singlet-triplet gap in Wurster's Blue Perchlorate for a pair of Wurster's cations. We lump together all the paired electrons on each molecule and the positive nuclei to form a core, and we consider the motion of the unpaired electrons in the potential field of these two cores and the field of their mutual electrostatic repulsion. We write the hamiltonian as follows:

$$\mathcal{H} = \mathcal{H}_{1a} + \mathcal{H}_{2b} + V_{1b} + V_{2a} + \frac{1}{r_{12}} \qquad (2)$$

$\mathcal{H}_{1a}$ and $\mathcal{H}_{2b}$ are the effective hamiltonians for a single core and its associated electron; V_{1b} and V_{2a} are the interaction potentials between one core and the other core's electron; $1/r_{12}$ is the electrostatic interaction between the two electrons. We consider zeroth order wave functions for the singlet and triplet states of the dimer to be appropriately normalized sum and difference functions of the solutions to the single core hamiltonians. We may then readily evaluate the singlet and triplet energies:

$$E' = \frac{1}{1+S_{ab}^2}\left\{\langle a_1 b_2 | \mathcal{H} | a_1 b_2\rangle + \langle a_1 b_2 | \mathcal{H} | a_2 b_1\rangle\right\}$$

$$E^3 = \frac{1}{1-S_{ab}^2}\left\{\langle a_1 b_2 | \mathcal{H} | a_1 b_2\rangle - \langle a_1 b_2 | \mathcal{H} | a_2 b_1\rangle\right\} \qquad (4)$$

where S_{ab} is the overlap between the two localized wave functions. Subtracting, and using the fact that the localized functions are solutions to the single core hamiltonians, we find for the singlet-triplet gap:

$$J = \frac{2}{1-S_{ab}^4}\left\{\langle a_1 b_2 | V_{1b} + V_{2a} + \frac{1}{r_{12}} | a_2 b_1\rangle - S_{ab}^2 \langle a_1 b_2 | V_{1b} + V_{2a} + \frac{1}{r_{12}} | a_1 b_2\rangle\right\} \quad (5)$$

We rewrite this as:

$$J = \frac{2}{1-S_{ab}^4}\left\{T_{ab} - S_{ab}^2 T_{aa} - 2S_{ab}Q_{ab} + 2S_{ab}^2 Q_{aa}\right\} \quad (6)$$

where T_{ab} is the actual two-electron exchange integral, T_{aa} is the two-electron coulomb integral, Q_{ab} is the exchange nuclear attraction integral, and Q_{aa} is the electron-other-core nuclear attraction integral. Equation 6 is used as the starting point for the calculation of J and J'. In this model J and J' are taken as the singlet-triplet gap for a near and far dimer, respectively.

III. The Calculation

The first step in the calculation of the singlet-triplet gap in WBP was to obtain reasonable solutions to the single core hamiltonian. McLachlan (6) has investigated the effect of hyperconjugation in free radicals and asserts that a simple Huckel calculation in which the coulomb and resonance integrals for nitrogen are chosen equal to those for carbon gives spin densities in better

agreement with experiment than those obtained from a more elaborate calculation. We therefore used the simplest calculation.

A computer program to calculate eigenvalues and eigenvectors of a real, symmetric matrix was adapted to the CalTech computation center system, and used to calculate the pi-electron wavefunctions for a single Wurster's cation. Since the exchange effect we are studying is one that weights the regions of space rather far removed from the nuclei, it was felt that the use of simple Slater-type functions, which are known to underestimate the tail of the wavefunction, would not be adequate. We used the best available Hartree-Fock wavefunctions expressed as linear combinations of four Slater orbitals as calculated by Roothaan (7). The Huckel wavefunction used and the carbon and nitrogen wavefunctions are given in the appendix.

During the summers of 1962 and 1963, the author in collaboration with Drs. Martin Karplus and I. Shavitt had written general computer programs for the evaluation of one-electron, one-, two-, and three-center energy integrals. Three center nuclear attraction integrals were evaluated by the gaussian transform technique originally proposed by Kikuchi (8) and used by Karplus and Shavitt (9) for the evaluation of two-electron integrals. These programs were modified to use Hartree-Fock

wavefunctions instead of Slater functions, and a control program to combine the calculated integrals into the singlet-triplet gap for a given atomic configuration was written.

We neglect the two-electron terms T_{ab} and T_{aa} primarily because of the lack of computer programs to evaluate them. This rather grotesque approximation may be slightly justified by noting that they must lead to stabilization of the triplet rather than the singlet, and, in the large distance approximation, cancel exactly. Of course, the other terms would also cancel in this approximation, but we may resort to a posteriori justification.

IV. Results

The first calculation, using the equilibrium configuration and nuclear charges shown in table 1, yielded a value for J of 56 cm^{-1}, almost a factor of five too low. The amount of alternation in spacing in the low temperature phase of WBP is unknown; we varied the inter-ring spacing (x-coord) and found that at a spacing of 0.5 Å less than in the high temperature phase we may match the experimental value. The variation of J with the inter-ring spacing is shown in figure 3. At a time when this calculation was thought fruitful, in the interest of saving computer time, we attempted to fit a "best" single Slater

function to the high temperature equilibrium value of J. The results of varying the exponent of this Slater function are shown in figure 4.

Further work on this problem would involve the inclusion of two-electron integrals in the expression for J and the use of considerably better wavefunctions for the single core solutions.

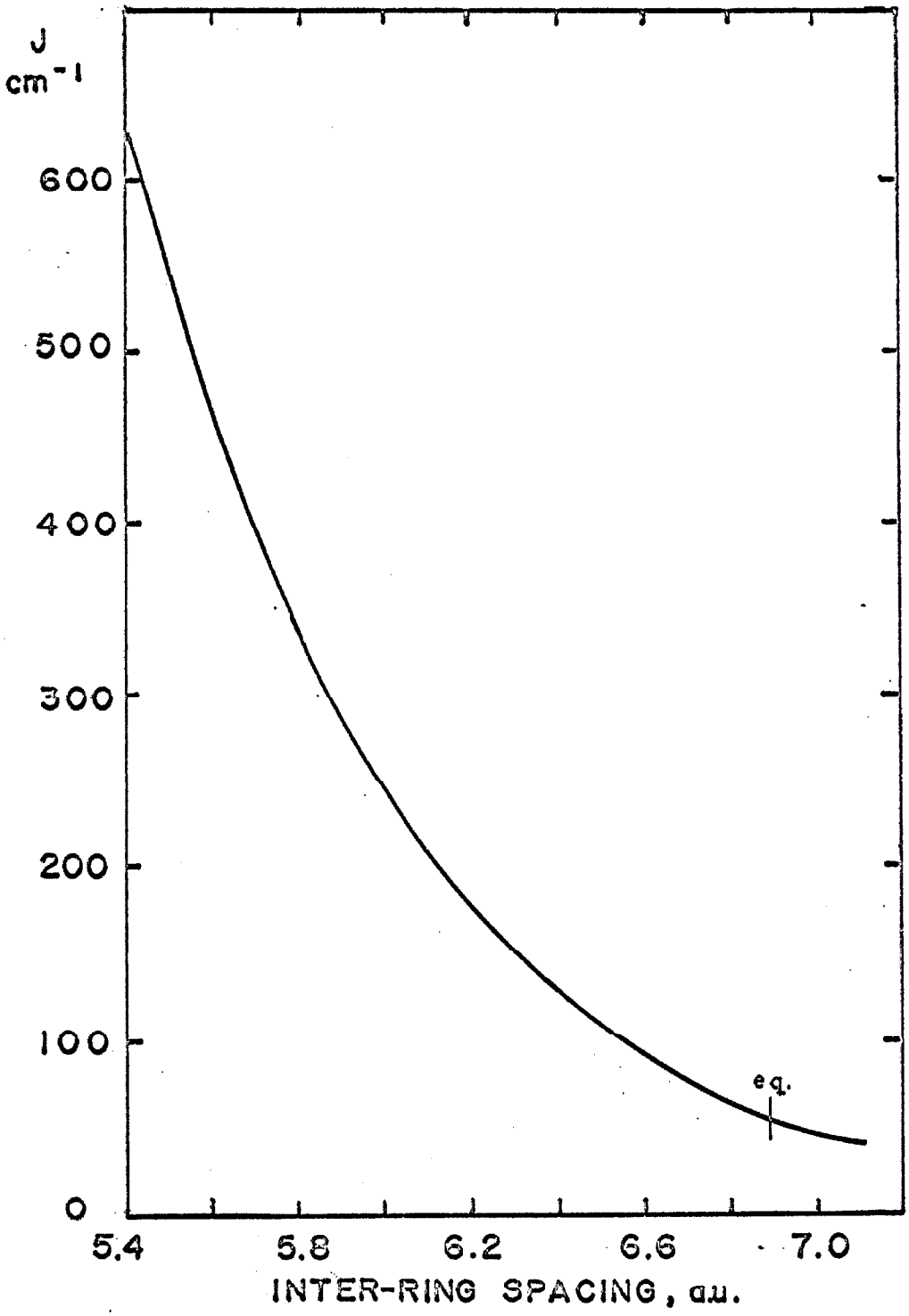

Fig. 3. Plot of J versus inter-ring spacing. The point marked "eq." is the high-temperature equilibrium point

Table 1. Coordinates and effective charges for a Wurster's dimer. Primed and unprimed numbers refer to molecules one and two respectively. Coordinates are expressed in atomic units.

Atom	x-coord.	y-coord.	z-coord.	Effective Charge
1N	0.	0.	0.	0.3323
2C	0.	-2.62	0.	0.0322
3C	0.	-3.95	2.25	0.0677
4C	0.	-6.55	2.25	0.0677
5C	0.	-7.88	0.	0.0322
6C	0.	-6.55	-2.25	0.0677
7C	0.	-3.95	-2.25	0.0677
8N	0.	-10.50	0.	0.3323
1'N	6.88	-1.62	0.	0.3323
2'C	6.88	0.97	0.	0.0322
3'C	6.88	2.29	2.25	0.0677
4'C	6.88	4.90	2.25	0.0677
5'C	6.88	6.22	0.	0.0322
6'C	6.88	4.90	-2.25	0.0677
7'C	6.88	2.29	-2.25	0.0677
8'N	6.88	8.85	0.	0.3323

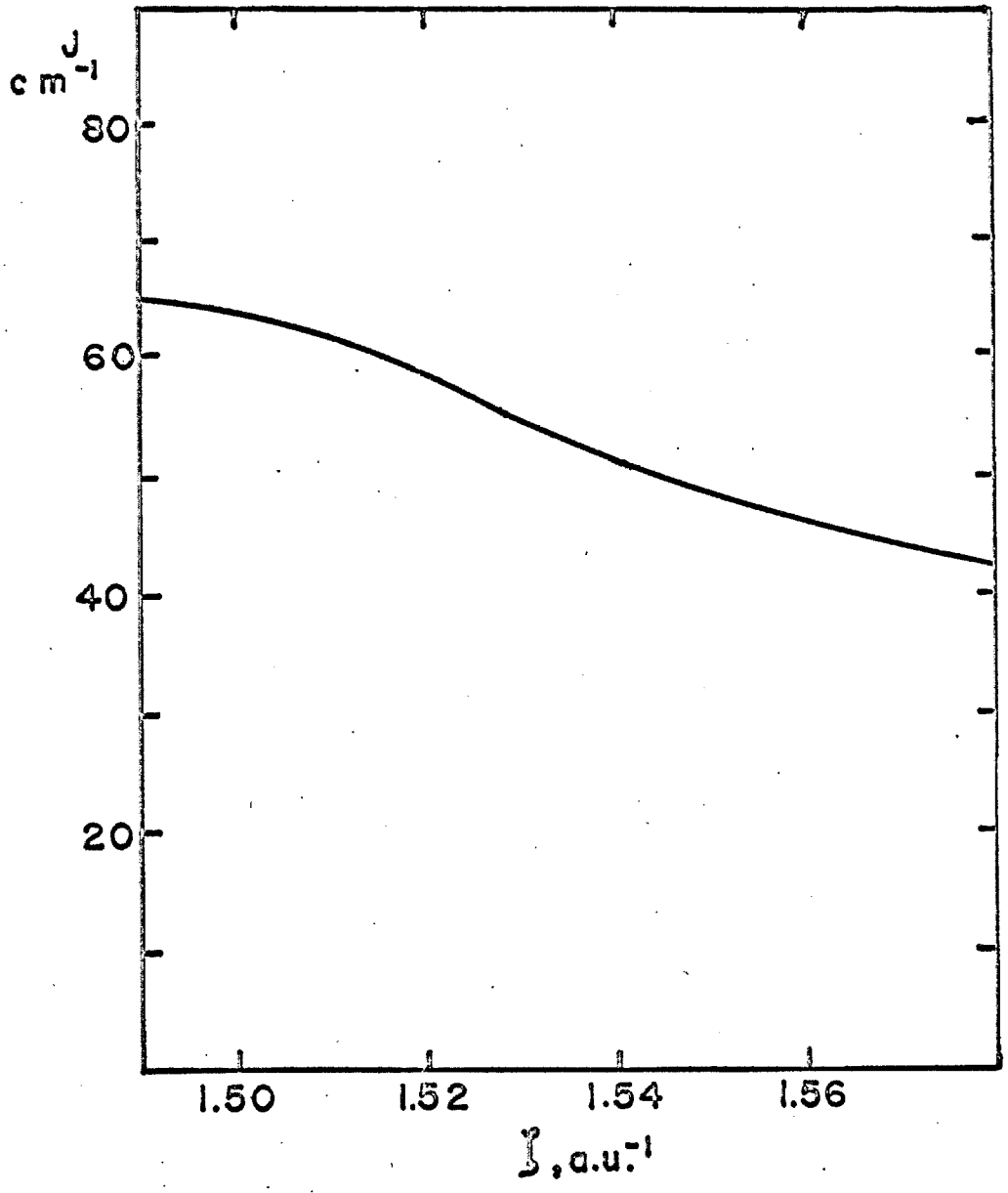

Fig. 4. Plot of J versus orbital exponent on nitrogen

Appendix

I. Huckel wavefunction used for the unpaired spin.

$$\psi = 0.57645\,|1N\rangle + 0.1793\,|2C\rangle - 0.2603\,|3C\rangle$$
$$-0.2603\,|4C\rangle + 0.1793\,|5C\rangle - 0.2603\,|6C\rangle$$
$$-0.2603\,|7C\rangle + 0.57645\,|8N\rangle$$

II. Self-consistent-field wavefunctions expressed in terms of Slater functions (7).

$$|iC\rangle = 0.24756\,\theta(0.95540) + 0.5773\,\theta(1.421) +$$
$$+0.23563\,\theta(2.5873) + 0.0109\,\theta(6.3438).$$

$$|iN\rangle = 0.2973\,\theta(1.1937) + 0.48388\,\theta(1.7124) +$$
$$+0.28079\,\theta(3.0112) + 0.01352\,\theta(7.1018).$$

$\theta(x)$ is a Slater 2-p orbital with orbital exponent x.

References

1. H. M. McConnell, D. Pooley and A. Bradbury, Proc. Nat. Acad. Sci. U.S., 48, 1480 (1962).

2. D. D. Thomas, H. Keller and H. M. McConnell, J. Chem. Phys., 39, 2321 (1963).

3. J. D. Turner and A. C. Albrecht, unpublished.

4. E. Hughes, private communication.

5. Zoltán G. Soos, private communication.

6. A. D. McLachlan, Mol. Phys., 1, 233 (1958).

7. C. C. J. Roothaan, J. Chem. Phys., 19, 1445 (1951).

8. R. Kikuchi, J. Chem. Phys., 22, 148 (1954).

9. I. Shavitt and M. Karplus, J. Chem. Phys., 38, 1256 (1963).

PROPOSITION II

The Use of the Gaussian Transform Method in Evaluating Multicenter Charge Moment Integrals

Abstract

The integral transform method for evaluating multicenter integrals between Slater orbitals is applied towards obtaining useful formulae for charge moment integrals.

I. Introduction

One of the major obstacles to a priori calculations in quantum chemistry has long been the difficulty in evaluating multicenter integrals. In 1954, Kikuchi (1) proposed that an integral transform, expressing Slater functions in terms of gaussian functions, be applied to this problem. The use of gaussian functions in quantum chemistry has long been considered (2) primarily because most of the three and four center integrals which are relatively intractable for Slater orbitals can be done analytically for gaussians. The major drawback to the use of gaussians is that they provide a relatively poor estimate of electron distributions: their radial dependence at large distances

seriously underestimates electron density. Boys (3) has attempted to use gaussian functions for molecular calculations, and has given formulae for the simplest energy integrals, that is, overlap kinetic energy, nuclear attraction, and inter-electronic repulsion integrals. Shavitt (4) was the first to realize the applicability of the integral transform method and has used it successfully to evaluate some of the more useful inter-electronic exchange and hybrid integrals. His final formulas are in terms of a threefold numerical integration which is quite amenable to computation with a computer. It is proposed that this method be used to evaluate charge moment integrals which are of use in the theory of crystal field splittings for molecules and the theory of electron scattering.

II. Integrals for Gaussian Orbitals

Since the transform we are going to use does not include normalization of the gaussian orbitals, we shall derive formulas only for unnormalized gaussian orbitals, given in equation 1.

$$G(\underline{r}_i, s_i) = \exp\{-s_i (r_i - r)^2\} \tag{1}$$

Also, since formulae for higher orbitals may be derived by elementary differentiation from formulae for 1S orbitals, we will derive formulas only for $1S^2$ type integrals (3).

We define R_n as the n^{th} charge moment integral between two unnormalized gaussian orbitals:

$$R_n = \int d^3r \exp\{-S_1(\underline{r}-\underline{r}_1)^2 - S_2(\underline{r}-\underline{r}_2)^2\} \cdot r_3^n \qquad (2)$$

where $\underline{r}_1$, $\underline{r}_2$, $\underline{r}_3$ are three distinct points in space, and the integral is taken over all space.

It is well known that the product of two gaussians may be expressed as a single gaussian, with orbital exponent equal to the sum of the two original exponents, and centered at a point somewhere on the line joining the two original points (to within a constant):

$$G(\underline{r}_1,S_1)\cdot G(\underline{r}_2,S_2) = K_{12}\, G(\underline{P}, S_1+S_2) \qquad (3)$$

where $$P_i = (S_1 r_{1i} + S_2 r_{2i})/S_1+S_2$$

$$K_{12} = \exp\left\{-r_{12}^2 \frac{S_1 S_2}{S_1+S_2}\right\}$$

By using this property of gaussians, we may readily express the charge moment integrals in terms of two basic types of integrals, one with finite limits, and one with infinite limits:

$$R_n = 2\pi K_{12} \int_0^\infty r_3^{n+2} dr_3 \int_{-1}^{1} d\cos\theta \exp -\{S(r_3^2 + P^2 + 2r_3 P\cos\theta)\} \qquad (4)$$

$$= \frac{\pi K_{12}}{SP} \int_0^\infty r_3^{n+1} dr_3 \left[\exp\{-S(r_3-P)^2\} - \exp\{-S(r_3+P)^2\}\right]$$

$$R_n = \frac{K_{12}\pi}{S\,P}\left\{\int_{-P}^{\infty}(r+p)^{n+1}\,dr\,e^{-Sr^2} - \int_{P}^{\infty}(r-p)^{n+1}\,dr\,e^{-Sr^2}\right\} \tag{5}$$

$$R_n = \frac{K_{12}\pi}{S\,P}\left\{\int_{0}^{\infty}(r+p)^{n+1} - (r-p)^{n+1}\,dr\,e^{-Sr^2} + \int_{-P}^{0}(r+p)^{n+1}\,e^{-Sr^2}\,dr \right. \tag{6}$$
$$\left. - \int_{P}^{0}(r-p)^{n+1}\,e^{-Sr^2}\,dr\right\}$$

In the above formulae S is the sum of s_1 and s_2, and p is the distance from r_3 to P (defined in eq. 3). We can further simplify by letting r go to -r in the second term of 6. Thus:

$$R_n = \frac{K_{12}\pi}{S\,P}\left[\int_{0}^{\infty}\left\{(r+p)^{n+1} - (r-p)^{n+1}\right\}e^{-Sr^2}\,dr + (-)^{n+1}\int_{0}^{P}(r-p)^{n+1}\,e^{-Sr^2}\,dr \right. \tag{7}$$
$$\left. + \int_{0}^{P}(r-p)^{n+1}\,e^{-Sr^2}\,dr\right]$$

$$R_n = \frac{K_{12}\pi}{S\,P}\left[\int_{0}^{\infty}\left\{(r+p)^{n+1} - (r-p)^{n+1}\right\}e^{-Sr^2}\,dr + \left(1+(-1)^{n+1}\right)\int_{0}^{P}(r-p)^{n+1}\,e^{-Sr^2}\,dr\right.$$

As a check on our juggling so far, we may let n = -1 in the above formula, giving the three center nuclear attraction integral:

$$R_{-1} = \frac{K_{12}\pi}{S\,P}\cdot 2\cdot\int_{0}^{P}\exp(-Sy^2)\,dr \tag{8}$$

which agrees with that given by Boys (3). If we were to expand $(r\pm p)^{n+1}$ by means of a binomial series, we find that all the terms we want can be expressed as:

$$A_{ij} = \frac{K_{12}\pi}{S_P} \int_0^\infty r^i p^j \exp(-Sr^2)\, dr \tag{9}$$

and

$$B_{ij} = \frac{K_{12}\pi}{S_P} \int_0^P r^i p^j \exp(-Sr^2)\, dr \tag{10}$$

where we have dropped certain uninteresting factors (constants). Having developed these preliminary results for gaussian orbitals, we are now in a position to consider the use of an integral transform expressing Slater orbitals as integrals over gaussian orbitals.

III. The Integral Transform Method

The required transform we want is a special case of a general integral representation of the reduced, modified Bessel functions (5).

$$k_m(ar) = \frac{1}{2}\left(\frac{a^2}{2}\right)^m \int_0^\infty s^{-m-1} \exp(-a^2/4s - sr^2)\, ds \tag{11}$$

For 1/2-integral values of m, these Bessel functions reduce to polynomials in ar multiplied by exp(-ar); in particular for m = 1/2 we find,

$$\exp(-ar) = \frac{1}{\sqrt{\pi}} \frac{a}{2} \int_0^\infty s^{-3/2} \exp(-a^2/4s - r^2 s)\, ds \tag{12}$$

We define the general charge moment integral:

$$Q_n = \int d^3r\, r_3^n \exp(-ar_1 - br_2)\, N_1 N_2 \tag{13}$$

where, as in the definition of R_n, the integral is over all space, and N_1 and N_2 are the normalization constants for the 1S Slater orbitals. Then, applying the transform of equation 12, we may express the Q_n as integrals over the corresponding R_n.

$$Q_n = \int_0^\infty ds_1 \int_0^\infty ds_2 (s_1 s_2)^{-3/2} \exp\left(-\frac{a^2}{4s_1} - \frac{b^2}{4s_2}\right) N_1 N_2 R_n \tag{14}$$

We have seen above that the R_n's may be expressed in terms of only the A_{ij} and the B_{ij}, so we will evaluate only those integrals in equation 14 where the R_n has been replaced by A_{ij} and B_{ij}.

We first consider the simpler of the two types of integrals, those over the B_{ij}. Recalling the definition of K_{12}, we note that K_{12} is a function of s_1 and s_2 and, therefore, may not be yanked out from under the integral sign. Defining Q_{ij}^B as the B_{ij} term in Q_n, we find,

$$Q_{ij}^B = \frac{N_1 N_2 ab}{2} \int_0^\infty ds_1 \int_0^\infty ds_2 (s_1 s_2)^{-3/2} \exp\left(-\frac{a^2}{4s_1} - \frac{b^2}{4s_2} - \frac{s_1 s_2}{s} r_{ab}^2\right) \cdot \tag{15}$$

$$\cdot \frac{1}{sp}\, p^i \int_0^p y^i\, dy \exp - sy^2$$

In order to simplify this appalling expression, we make the shrewd change of variables $z = s_1+s_2$ and $u = s_1/(s_1+s_2)$; in terms of the new variables, the old are expressed as $s_1 = zu$ and $s_2 = z(1-u)$. The Jacobian of this transformation, $J(s_1,s_2/z,u)$, is readily evaluated as z. The range of z is from 0 to ∞, while the range of u is from 0 to 1. In terms of these new variables, we may now express Q_{ij}^B as:

$$Q_{ij}^B = N_1N_2\frac{ab}{2}\int_0^1 du\int_0^\infty dz(z)z^{-3}\{u(1-u)\}^{-3/2}\exp\left[-\frac{1}{2}\left(\frac{a^2}{4u}+\frac{b^2}{4(1-u)}\right)\right]\cdot$$
$$\cdot p^{\frac{1}{2}}z\exp\left[-z\,u(1-u)r_{ab}^2\right]\int_0^p p^j q^i \exp -zq^2\,dq \qquad (16)$$

$$= N_1N_2\frac{ab}{2}\int_0^1 du\,\frac{1}{[u(1-u)]^{3/2}}\,p^{j+i}\int_0^1 x^i dx\int_0^\infty \frac{dz}{z^3}\cdot$$
$$\cdot\exp\left\{-z\left[u(1-u)r_{ab}^2+p^2x^2\right]-\frac{1}{2}\left[\frac{a^2}{4u}+\frac{b^2}{4(1-u)}\right]\right\}$$

where we have used the transformation $x = y/p$ in obtaining the second equality. We now observe that the integral over z in equation 16 is of the general form of equation 11. We define some sundry constants, and then perform the z integral:

$$\sigma = \frac{1}{p^2}\left(u(1-u)r_{ab}^2\right) \qquad (17)$$

$$\tau = p^2 \cdot \frac{1}{4} \left\{ \frac{a^2}{u} + \frac{b^2}{1-u} \right\} \tag{18}$$

$$Q_{ij}^{\beta} = \int_0^1 du \int_0^1 x^i dx \; p^{j+i} \frac{2p^4}{(2\tau)^2} k_2\left(2\sqrt{\tau(\sigma+x^2)}\right) \frac{(ab)^{5/2}}{2\pi} \tag{19}$$

In equation 19, we have already expanded the normalization constants for the Slater orbitals. Equation 19 now expresses the charge moment integrals, or rather part of them, in a form which is quite amenable to solution on a computer. For the particular case of i a multiple of 2, the x integration may be performed in terms of some special functions, the $T_{m,n}$ functions which appear in Shavitt's expression for the four-center exchange integrals. The major difference between our expression and his is that our expression involves modified Bessel functions of integral order, which lead to $T_{m,n}$ of half-integral m, while Shavitt's formulae involve half-integral Bessel functions, and, therefore, $T_{m,n}$ of integral m. However, many of the formulae that Shavitt has derived for series expansions, asymptotic expansions, and recursion relations of the $T_{m,n}$ (6) may be carried over to the case of half-integral m. In collaboration with Drs. Shavitt and Karplus, the author has written computer programs for the evaluation of these $T_{m,n}$ functions of half-integral m. In general, since the

final result involves only a twofold integral, the most straightforward method of evaluating these functions, by Gauss-Legendre quadrature, has been found to be sufficiently fast and accurate for most purposes, in particular, the evaluation of three-center nuclear attraction integrals.

We have now reduced half of our integrals to a form adaptable to computer evaluation; we shall now go on to consider the other type of integral, that involving the functions A_{ij} as defined in equation 9.

In a manner completely analogous to that used in the previous derivation of the Q^B_{ij}, we define Q^A_{ij}, perform the same transformation of variables, and after doing the z integration, we obtain the following formula for the Q^A_{ij}:

$$Q^A_{ij} = \int_0^1 du \int_0^\infty x^i dx\, p^{1+i+q} \frac{2}{(2\tau)^2} \frac{(ab)^{5/2}}{2\pi} k_2(2\sqrt{\tau(\sigma+x^2)}) \qquad (20)$$

We will apparently have no trouble with the u integration, but we must investigate the convergence properties of the x integral. For this, we look at the expansion of $k_m(x)$ for large x (7):

$$k_m(x) \sim x^m \sqrt{\frac{\pi}{2x}} \exp -x \qquad (21)$$

Thus, at large x, the integrand goes as $x^{m+i-1/2}e^{-x}$, which is quite a decent function. Therefore, we will have no trouble evaluating the x integral. We may either use

Gauss-Laguerre integration quadrature, or make the elementary change of variables y = x/1+x, which will convert the integral to one between the limits of 0 and 1, and use Gauss-Legendre quadrature.

It is encouraging to note at this point, that if we set n = -1 and attempt to evaluate Q_1, the only term which survives is the B_{oo} term; we plug into our formulae and obtain for the three-center nuclear attraction integral:

$$Q_{-1} = (ab)^{5/2}/\sqrt{\pi} \int_0^1 du\, [u(1-u)]^{-3/2} p^4 T_{5/2,o} \qquad (22)$$

which is equivalent to the formula stated, but not derived by Shavitt (8).

We have only derived formulae for $1S^2$ integrals so far; formulae for higher orbitals can be obtained from elementary differentiation. We note that each differentiation with respect to the orbital exponent brings down a factor of r_1, while differentiation with respect to the x-, y-, and z-coordinates of the i^{th} nucleus brings down a factor of the orbital exponent times the x-, y-, and z-coordinates. Thus, by applying these differentiations under the integral signs in equations 19 and 20, we may obtain formulae for higher Slater orbitals. Shavitt (9) has written a computer program, which given the formula for the $1S^2$ integral will generate formulae for higher orbitals, through 3d.

IV. Conclusion

We have seen that the application of the integral transform of equation 12 has enabled us to reduce the problem of evaluating three-center charge moment integrals to the relatively simple task of performing a twofold numerical integration over reduced, modified, Bessel functions. The utility of the method lies in the fact that the product of two gaussians on different centers is expressible as a constant times a gaussian on a third center. Thus, we may convert a rather difficult threefold space integration over infinite limits to a much simpler twofold integration over finite limits.

The author would like to thank Dr. Isaiah Shavitt for providing him with a preprint of his chapter on gaussians from Methods in Computational Physics.

References

1. Kikuchi, J. Chem. Phys., 22, 148 (1954).

2. For a review of the use of gaussian functions in quantum chemistry see Harris, Rev. Mod. Phys., 33, 558 (1963), and Shavitt, "The Gaussian Function in Calculations of Statistical Mechanics and Quantum Mechanics," in Alder, Fernbach and Rotenberg (eds.), Methods in Computational Physics, Vol. 2 (New York: Academic Press, 1963).

3. Boys, Proc. Roy. Soc. (London), A200, 542 (1950).

4. Shavitt, op. cit., and Shavitt and Karplus, J. Chem. Phys., 36, 550 (1962).

5. Shavitt, op. cit., equations 55-59.

6. Ibid., equations 119-135.

7. Watson, Theory of Bessel Functions (New York: Macmillan, 1948), p. 202.

8. Shavitt, op. cit., equation 140, with inclusion of normalization constants.

9. Ibid., equations 143-152.

PROPOSITION III

Isolated Electron Model for Zero-field Parameters

Abstract

A simple model for the calculation of zero-field splittings in triplet states which may be thought of as biradicals is proposed. This method may be used to estimate the amount of charge transfer present in the triplet state.

I. Introduction

The electron paramagnetic resonance (EPR) spectrum of organic triplets has been under considerable study recently (1). Since the early work of Hutchison and Mangum (2), much work has been done on the spin-spin interaction in these triplet states. From measurements of the principal axis splittings at high field as well as the zero-field resonance frequencies themselves, one may determine the energies of the three zero-field states.

The hamiltonian for the spin-spin interaction in such triplets may be written:

$$\mathcal{H} = g^2\beta^2 \frac{1}{r_{12}^3} \underline{S}_1^{\dagger} \cdot (\underline{\underline{1}} - 3\hat{\underline{r}}\hat{\underline{r}}) \cdot \underline{S}_2 \qquad (1)$$

where $\underline{s}_1$ and $\underline{s}_2$ are the spin operators for electrons 1 and 2 respectively and $\underline{r}_{12}$ is the vector distance between them. It is rather easy to show that this hamiltonian may be written as:

$$\mathcal{H} = D(S_z^2 - \tfrac{1}{3}\underline{S}^2) + E(S_x^2 - S_y^2) \qquad (2)$$

where x, y, and z are the principal axes for the particular molecule under consideration. In this coordinate system, with the use of appropropriate values for D and E one may show that the matrix representations of the hamiltonians 1 and 2 are identical. In fact, Silverstone (3) has shown that a "D and E" hamiltonian may be used to represent states of higher multiplicity.

II. The Model

We now consider the isolated electron model for the calculation of D and E. For certain types of molecules, such as Wurster's Blue Perchlorate (WBP) or some of the TCNQ compounds (4) two of the doublet monomers dimerize in the crystal state to form a singlet ground state and a triplet excited state. The zero-field parameters of these compounds have been determined. Since the bonding interaction in these compounds is not very large, one may hope that the two electrons whose spins form the triplet state may be considered to be independent. If this is so, we may write the hamiltonian as:

$$\mathcal{H} = g^2\beta^2 \underline{S}_1^{\dagger} \cdot \left\{ \sum_{\substack{\alpha \in A \\ \beta \in B}} \frac{\rho_\alpha \rho_\beta}{r_{\alpha\beta}^3} \left(\underline{\underline{1}} - 3 \hat{r}_{\alpha\beta} \hat{r}_{\alpha\beta} \right) \right\} \cdot \underline{S}_2 \qquad (3)$$

where the rhos are the spin densities for the two electrons at the sites of the atoms α and β . The two electrons of course must not share any common atom. Using this formula and the experimental spin densities (or those calculated from a Huckel approximation) one may easily evaluate the spin hamiltonian matrix, and diagonalize it to obtain the parameters D and E. A computer program has been written to perform this calculation and used to evaluate D and E for a few crystals.

For WBP the experimental values are: D = 0 MH; E = 212$\pm$6 MH (5); the theoretical values are: D = -13 MH; E = 236 MH.

For Morpholinium TCNQ we find

Experiment: D = 450 MH; E = 54 MH (6);

Theory: D = 463 MH; E = 44 MH.

We have also used this method to evaluate the zero-field parameters for the peculiar compound bis(2,2'-diphenylene) methane. This compound has been studied experimentally (7) and has a dinegative ion with what is believed to be a ground triplet state. Using spin densities given by simple Huckel theory for the biphenyl negative ion, and assuming the molecule to have one electron localized on each of the

biphenyl groups, we obtain values of D and E which are equivalent to those obtained from assuming two point electrons about 6.57 Å apart, in excellent agreement with the experimental value of 7 Å for the mean interatomic distance.

Thus we see that for dimeric systems it is often possible to regard the triplet state as a biradical with one spin on each monomer, and use this approximation to calculate the zero-field splitting in the triplet. The deviation of our calculated value from the experimental value should be a measure of the importance of charge-transfer in the triplet state.

References

1. a) M. S. DeGroot and J. H. Van der Waals, Mol. Phys., 6, 545 (1964).

   b) N. Hirota and C. A. Hutchison, Jr., J. Chem. Phys., 42, 2896 (1965).

2. C. A. Hutchison, Jr. and B. W. Mangum, J. Chem. Phys., 34, 908 (1961).

3. H. J. Silverstone, Thesis, California Institute of Technology (1964).

4. D. D. Thomas, A. W. Merkl, A. F. Hildebrandt, and H. M. McConnell, J. Chem. Phys., 40, 2588 (1963).

5. D. D. Thomas, H. Keller, and H. M. McConnell, J. Chem. Phys., 39, 2321 (1963).

6. M. A. Maréchal and H. M. McConnell, J. Chem. Phys., 43, 497 (1965).

7. R. D. Cowell, G. Urry and S. I. Weissman, J. Chem. Phys., 38, 2028 (1963).

PROPOSITION IV

Anomalous Linewidths in Biradical Spectra

Abstract

The effect of an exchange interaction between two spins in a biradical is examined. It is proposed that the alternation in linewidth of the five hyperfine lines in nitroxide biradicals may be explained as the breakdown of the usual assumption that $J \gg a$. The line broadening calculated for the case of $J \ll a$ is also given. The results here obtained are contrasted with those of Luckhurst (1). An experiment to distinguish between the two theories is proposed.

I. Introduction

In a recent paper, Luckhurst has proposed a theory for alternating linewidths of nitroxide biradicals in the presence of a strong exchange coupling between the two spins (1). By making the assumption that the exchange interaction is very much larger than the hyperfine interaction, and that the exchange interaction is modulated by

conformational isomerization in solution, he applies the theory of Redfield (2) and shows that the two central lines in the five-line hyperfine pattern should be broadened more by this modulation than the central and outside lines. We propose that a much simpler explanation is adequate. We will calculate the shifts in the various hyperfine lines for the case where the hyperfine frequency is not negligible compared to the exchange frequency, and show that the result of Luckhurst obtains. We will also consider the other limit where the hyperfine interaction dominates the exchange interaction.

II. Theory in the Exchange Dominant Limit

We first write down the hamiltonian for a nitroxide biradical in the presence of an exchange interaction between the two spins. We are considering solution spectra where the hyperfine and g-tensors may be assumed isotropic. For this case the hamiltonian for a single radical may be written:

$$\mathcal{H}_1 = g\beta \underline{H}^{\dagger} \cdot \underline{S}_1 + a\, \underline{S}_1^{\dagger} \cdot \underline{I}_1 \qquad (1)$$

where *a is the isotropic hyperfine coupling constant* between the spin 1/2 electron and the spin 1 nitrogen nucleus, g is the isotropic g factor for the electron, and $\underline{H}$ is the external magnetic field. We write the hamiltonian for the

biradical as the sum of the two single radical contributions plus an exchange term:

$$\mathcal{H} = \mathcal{H}_1 + \mathcal{H}_2 + J\,\underline{S}_1 \cdot \underline{S}_2 \tag{2}$$

The biradical system is a thirty-six state system, and we may write down the states that are connected by the exchange interaction directly. For each orientation of the two magnetic nuclei, there are four states with differing values of the electron spin z-component.*

The exchange interaction connects two of these four states (those two with opposite electron spins) and connects no two states with different values of the nuclear quantum numbers. We may write the secular determinant for these two-state manifolds that are affected by the exchange interaction as:

$$\begin{vmatrix} E_x - J/4 - E & J/2 \\ J/2 & -E_x - \frac{J}{4} - E \end{vmatrix} \tag{3}$$

where E_x is the energy of the state with electron one up and electron two down when the exchange vanishes. We solve immediately for the two energies:

$$E = -J/4 \pm \sqrt{E_x^2 + J^2/4} \tag{4}$$

---

*Spin quantization is along the direction of the external field.

In the limit of $a \ll J$ we expand the square root and obtain:

$$\varepsilon \approx -J/4 \pm J/2 \pm a^2/J \tag{5}$$

We need consider only the upper sign of equation 5, since for the lower sign the electron spin function is a singlet state, and has no magnetic transitions. From these energies we may obtain the shifts for the eighteen components of the spectrum.

Six of the components, two each at hyperfine frequencies a, 0, -a are unaffected. Of the four other transitions at hyperfine frequency 0, two are shifted up-field by a^2/J and two are shifted down-field by the same amount. All four of the transitions at $\pm a/2$ are shifted. Two are shifted up-field by $a^2/4J$ and two down-field. So we see that in this limit the $\pm a/2$ lines are effectively broadened by $a^2/2J$ while the outside lines are unaffected. The central line presents somewhat more of a problem. Part of it, with intensity equal to the intensity of the outside lines, is unaffected. The other two-thirds of the intensity should be shifted by $\pm 2a^2/J$ by the exchange interaction. If we assume that this shift, four times the shift of the a/2 lines, is sufficient so that the lines are distinct from the center line, and in fact disappear into the wings of the a/2 lines, the experimental spectrum as shown in (1) is reproduced (see figure 1 (a)). This anomalous shift is

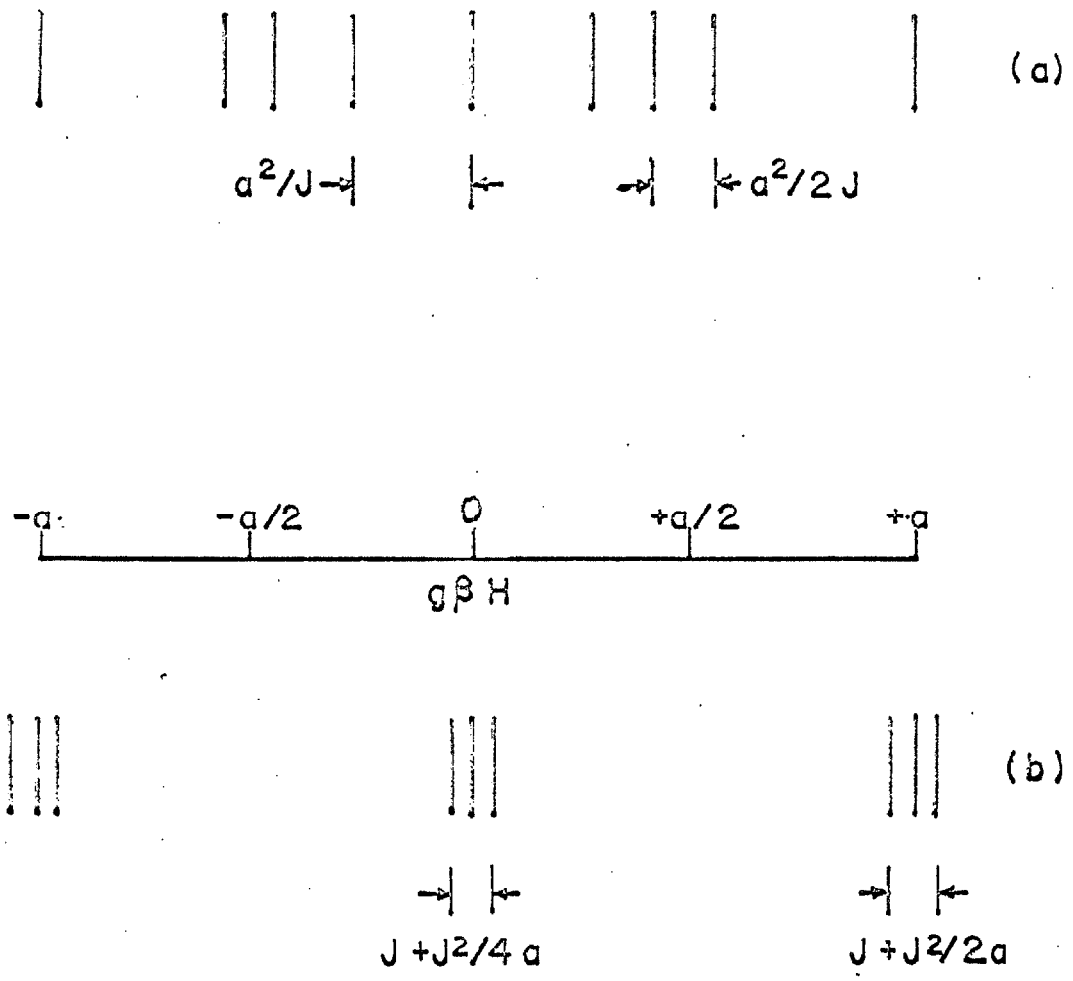

Fig. 1. Stick spectra for nitroxide biradicals
(a) Exchange dominant
(b) Hyperfine dominant

not surprising, since the observed width of the a/2 lines is not much smaller than the splitting, and, in fact, the five lines are not particularly well resolved.

III. Theory in the Hyperfine Dominant Limit

If we consider the hyperfine term to be much larger than the exchange term in the square root of equation 4, we may again expand the square root and obtain for the energies:

$$E = -\frac{J}{4} \pm E_x \pm J^2/8E_x \qquad (E_x \neq 0)$$

or

$$E = +J/4\ ,\ -3J/4 \qquad (E_x = 0) \tag{6}$$

If we now use these energies to calculate the spectrum we see that the three line spectrum in the absence of exchange is broadened by the exchange interaction. The central line is broadened by $J/2+J^2/8a$; the two outside lines are broadened by $J/2+J^2/4a$. As we first "turn on" the exchange interaction, the three lines broaden equally. As the interaction becomes stronger and stronger, the outside lines are first broadened more than the inside line (figure 1 (b)), then begin to narrow as the outermost component of each begins to move in to become part of the a/2 line (when the molecule can be considered to be in a triplet state).

IV. Conclusion

We have seen that we may calculate the anomalous linewidths for nitroxide biradicals by a very simple scheme. Our scheme gives results which agree with the experimental work of Luckhurst, and the more complicated relaxation theory he proposes. An experiment which would serve to distinguish between these two theories would be one which measures the temperature dependence of the broadening. If the only effect on the spectrum can be assumed to be from the exchange interaction and its modulation, if Luckhurst's theory is applicable, an increase in temperature should always serve to broaden the lines, since motion and hence the modulation of the exchange interaction should always increase. If our theory is right, the broadening should be almost independent of temperature, since it depends entirely on static properties.

References

1. G. R. Luckhurst, Mol. Phys., 10, 543 (1966).
2. A. G. Redfield, I.B.M.J. Res. Develop., 1, 19 (1957).

PROPOSITION V

Superconductive Matrix Element in Metals with Molecular Impurities

Abstract

We calculate the superconductive matrix element in metals doped with molecular impurities. Closed-form expressions are obtained for homonuclear diatomic molecules. The extension of the formalism to molecules whose electrons can be represented by LCAO wavefunctions is discussed.

I. Introduction

Since the discovery of superconductivity in mercury by Kammerlingh Onnes in 1911 (1), much work has been directed towards the construction of an adequate microscopic theory for this phenomenon (2). The first proposal with any degree of success was that of Fröhlich (3) who suggested that the basic interaction responsible for superconductivity was a phonon-coupled interaction between two electrons in the conduction band of a metal. Since his work, Bardeen, Cooper and Schrieffer (4) have put the phonon-coupled interaction on a more firm

theoretical basis, and have developed a theory which successfully accounts for the superconducting transition in many metals. However, there are some metals for which this theory is woefully inadequate, and mechanisms other than the phonon-coupled interaction must be assumed.

Recently, Hoffman (5) has reported some experimental work in which thin films of vanadium and indium are prepared, and a film of molecular impurity is deposited on them. It is found that for an appropriate choice of molecule, the superconducting transition temperature is raised. We here propose a theory, quite parallel to the development of the phonon-coupled interaction in most superconductors, which will hopefully apply to this system.

II. Theory for a Homonuclear Diatomic Molecule

We will consider a distribution of molecules in a metallic lattice where each of the molecules is at one of the set of points $\{R_\ell\}$. For simplicity, we first consider molecules in which there is only one excited state of importance. We let the interaction potential between conduction electrons and the molecular electrons be screened:

$$V = \frac{e^2}{r_{12}} \exp(-\mu r_{12}) \tag{1}$$

We neglect the nuclei, as they may be treated by the theory of Langer and Vosko (6) for point impurities in metals. We write a two-electron wavefunction for the metal in the presence of the molecular impurity to first order

$$|k_1,k_2\rangle = |k_1,k_2,0\rangle + \sum_{k_1',R_\ell} |k_1',k_2,R_\ell\rangle \frac{M(k_1'-k_1,R_\ell)}{E^0_{k_1}-E^0_{k_1'}-E_m} + (k_1 \leftrightarrow k_2) \qquad (2)$$

where the first two quantum numbers are the wave vectors of electrons one and two respectively, and the third is the location of the excited molecule. $M(k_1'-k_1,R_\ell)$ is the matrix element for the inelastic scattering of a single electron from state k_1' with excitation of the molecule at R_ℓ. E_m is the molecular excitation energy. The second term is the equivalent of the first with scattering of electron two instead of one. Using these wavefunctions, we may evaluate the effective matrix element between two-electron states in the metal:

$$\langle k_1,k_2|\tilde{V}|k_1',k_2'\rangle = \sum_{R_\ell} \left\{ \frac{2M(k_1'-k_1,R_\ell)M^*(k_2'-k_2,R_\ell)E_m}{(E_{k_1}-E_{k_1'})^2-E_m^2} + \begin{pmatrix} k_1 \leftrightarrow k_2 \\ k_1' \leftrightarrow k_2' \end{pmatrix} \right\} \qquad (3)$$

Our purpose here is to evaluate this matrix element for various molecules. We first consider homonuclear diatomic molecules, where the ground state wavefunction may be thought of as a sum of Slater orbitals at the two nuclei, and the excited state wavefunction as the difference

of these functions. We may then write M as the product of some normalization factors and two integrals:

$$M(K,R_\ell) = \frac{e^2}{2V\sqrt{1-S^2}}\, I_1 I_2 \tag{4}$$

where the integrals I_1 and I_2 are defined by:

$$\begin{aligned} I_1 &= \int d^3 r_{12}\, \exp(-i\vec{K}\cdot\vec{r}_{12} - \mu r_{12})/r_{12} \\ I_2 &= \int d^3 r_2\, \exp(-i\vec{K}\cdot\vec{r}_{12})\{\psi_A^2(2) - \psi_B^2(2)\} \end{aligned} \tag{5}$$

ψ_A and ψ_B are the Slater functions for the electron on atoms A and B respectively.

The integral I_1 is trivial:

$$I_1 = 4\pi/(K^2+\mu^2) \tag{6}$$

Insertion of a Slater orbital with exponent $\zeta/2$, and a fair amount of tedious algebra leads to the value for I_2:

$$I_2 = \frac{2\zeta^4 i}{(\zeta^2+K^2)^2}\exp(-i\vec{K}\cdot\vec{R}_\ell)\sin\tfrac{\rho}{2}\hat{K}\cdot\hat{r}_\ell \tag{7}$$

where ρ and $\hat{r}_\ell$ are defined by:

$$\begin{aligned} R_{A\ell} &= R_\ell - \tfrac{\rho}{2}\hat{r}_\ell \\ R_{B\ell} &= R_\ell + \tfrac{\rho}{2}\hat{r}_\ell \end{aligned} \tag{8}$$

We may run a quick dimensional check on our final expression for M and find that it is indeed in terms of energy. We also note that:

$$M(K,R) = M^*(-K,R) \tag{9}$$

III. Extension to More Complicated Molecules

The most elementary extension to the calculation above is to use Slater functions other than 1S. This is rather trivial to do, if one uses the recursion relation between the various orbitals and their derivatives (7).

We will consider the extension to various other molecules where the ground and excited state wavefunctions may not be considered as sum and difference functions. If the two states are written

$$\psi_1 = \sum \alpha_i \chi_i(r)$$
$$\psi_2 = \sum \beta_i \chi_i(r) \tag{10}$$

where the chi's are simple Slater functions at the various nuclei, we may write for M:

$$M = I_1 \left(\sum_{i,j} \alpha_i^* \beta_j \Lambda_{ij} \right) \frac{1}{V} \tag{11}$$

where Λ_{ij} is an integral:

$$\Lambda_{ij} = \int d^3r \exp(-i\vec{\kappa}\cdot\vec{r}) \chi_i^*(r) \chi_j(r) \tag{12}$$

We now apply ourselves to the solution of this integral. We first make the standard transformation:

$$\xi = r_1 + r_2 / R$$
$$\eta = r_1 - r_2 / R \tag{13}$$
$$\varphi = \varphi$$

where R is the distance between the two nuclei. We will consider only 1S orbitals, formulae for higher orbitals being derivable from these by differentiation. We substitute for the orbitals, define θ_k and φ_k as the spherical coordinates of the scattering vector in the molecular coordinate system, and obtain for Λ_{ij}:

$$\Lambda_{ij} = \frac{N_i N_j R^3}{8} \int_1^\infty d\xi \int_{-1}^{1} d\eta \int_0^{2\pi} d\varphi \; e^{-\rho\xi - \tau\eta} \exp\left[-ikR \frac{\xi+\eta}{2} \left\{ \frac{1+\xi\eta}{\xi+\eta} \cos\theta_k + \cos\varphi \varphi_k \sin\theta_k \cdot \frac{\sqrt{(1-\eta^2)(\xi^2+1)}}{\xi+\eta} \right\} \right] \tag{14}$$

where:

$$\rho = \left(\zeta_i \frac{+}{2} \zeta_j \right) \cdot R \qquad \tau = \left(\frac{\zeta_i - \zeta_j}{2} \right) R \tag{15}$$

N_i, N_j are normalization constants.

We now observe that the phi integration may be performed to give a zero order Bessel function of the first kind, and the xi integral may be thrown into the form of a Hankel transform; doing these two integrals we obtain for Λ_{ij}:

$$\Lambda_{ij} = N_i N_j \frac{\rho^3}{8} \cdot 2\pi e^{i\gamma} \int_{-1}^{1} d\eta \; \exp -\tau\eta \; \left\{ \pi(0,2) - (1-\eta^2)\pi(0,0) \right\} \tag{16}$$

where, as usual, we have introduced a host of new symbols:

$$\gamma = -\frac{kR}{2}\cos\theta_k \qquad \delta = -\frac{k\rho}{2}\sin\theta_k$$

$$y = \delta\sqrt{1-\eta^2} \qquad \mu = \rho - i\gamma\eta \tag{17}$$

$$\pi(n,m) = \int_0^\infty \sqrt{u}\, du \; J_n(uy) \frac{u^{m+1/2}}{\sqrt{1+u^2}} \exp -\mu\sqrt{1+u^2}$$

We note that the integrals, $\pi(n,m)$ are found in tables (8) for n=m:

$$\pi(m,m) = \sqrt{\frac{2}{\pi}} \frac{y^m}{(\mu^2+y^2)^{2m+1/4}} K_{m+1/2}(\sqrt{\mu^2+y^2}) \tag{18}$$

and for n≠m may be obtained by recursion:

$$\frac{\partial}{\partial y} \pi(n,m) = \frac{1}{2} \{ \pi(n-1,m+1) - \pi(n+1,m+1) \} \tag{19}$$

The K's above are the modified Bessel functions of the second kind; the π's are functions of one argument (y) and one parameter (μ).

We are now left with a single integral over eta, which may be done by any standard quadrature method.

In conclusion, we note that we have obtained expressions for the superconductive matrix element for a metal with molecular impurities. By a self-consistent treatment of these matrix elements we should be able to calculate the transition temperatures for the system.

References

1. H. Kammerlingh Onnes, Comm. Phys. Lab. Univ. Leiden, 119, 120, 122 (1911).

2. See, for example, Blatt, Theory of Superconductivity (New York: Academic Press, 1964).

3. H. Fröhlich, Phys. Rev., 74, 845 (1950).

4. J. Bardeen, L. N. Cooper and J. R. Schrieffer, Phys. Rev., 108, 1175 (1957).

5. Brian Hoffman, Thesis, California Institute of Technology (1966).

6. J. Langer and S. Vosko, J. Phys. Chem. Solids, 12, 196 (1959).

7. See, for example, the article by Shavitt in Methods of Computational Physics, Vol. 2, ed. B. Alder (New York: Academic Press, 1963).

8. A. Erdelyi, W. Magnus, F. Oberhettinger and F. G. Tricomi, Tables of Integral Transforms, Vol. 2 (New York: McGraw-Hill, 1954), p. 31.